arXiv:1412.6663v3 [hep-ex] 23 Apr 2015

EUROPEAN ORGANISATION FOR NUCLEAR RESEARCH (CERN)

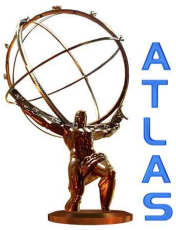

CERN-PH-EP-2014-274

Submitted to: JHEP

Search for charged Higgs bosons decaying via $H^{\pm} \to \tau^{\pm}\nu$ in fully hadronic final states using pp collision data at $\sqrt{s} = 8$ TeV with the ATLAS detector

The ATLAS Collaboration

Abstract

The results of a search for charged Higgs bosons decaying to a τ lepton and a neutrino, $H^{\pm} \to \tau^{\pm}\nu$, are presented. The analysis is based on 19.5 fb^{-1} of proton–proton collision data at $\sqrt{s} = 8$ TeV collected by the ATLAS experiment at the Large Hadron Collider. Charged Higgs bosons are searched for in events consistent with top-quark pair production or in associated production with a top quark, depending on the considered $H^{\pm}$ mass. The final state is characterised by the presence of a hadronic τ decay, missing transverse momentum, b-tagged jets, a hadronically decaying W boson, and the absence of any isolated electrons or muons with high transverse momenta. The data are consistent with the expected background from Standard Model processes. A statistical analysis leads to 95% confidence-level upper limits on the product of branching ratios $\mathcal{B}(t \to bH^{\pm}) \times \mathcal{B}(H^{\pm} \to \tau^{\pm}\nu)$, between 0.23% and 1.3% for charged Higgs boson masses in the range 80–160 GeV. It also leads to 95% confidence-level upper limits on the production cross section times branching ratio, $\sigma(pp \to tH^{\pm}+X) \times \mathcal{B}(H^{\pm} \to \tau^{\pm}\nu)$, between 0.76 pb and 4.5 fb, for charged Higgs boson masses ranging from 180 GeV to 1000 GeV. In the context of different scenarios of the Minimal Supersymmetric Standard Model, these results exclude nearly all values of $\tan\beta$ above one for charged Higgs boson masses between 80 GeV and 160 GeV, and exclude a region of parameter space with high $\tan\beta$ for $H^{\pm}$ masses between 200 GeV and 250 GeV.

© 2015 CERN for the benefit of the ATLAS Collaboration.

Reproduction of this article or parts of it is allowed as specified in the CC-BY-3.0 license.

Prepared for submission to JHEP

Search for charged Higgs bosons decaying via $H^{\pm} \to \tau^{\pm}\nu$ in fully hadronic final states using pp collision data at $\sqrt{s} = 8$ TeV with the ATLAS detector

The ATLAS Collaboration

Abstract: The results of a search for charged Higgs bosons decaying to a τ lepton and a neutrino, $H^{\pm} \to \tau^{\pm}\nu$, are presented. The analysis is based on 19.5 fb^{-1} of proton–proton collision data at $\sqrt{s} = 8$ TeV collected by the ATLAS experiment at the Large Hadron Collider. Charged Higgs bosons are searched for in events consistent with top-quark pair production or in associated production with a top quark, depending on the considered $H^{\pm}$ mass. The final state is characterised by the presence of a hadronic τ decay, missing transverse momentum, b-tagged jets, a hadronically decaying W boson, and the absence of any isolated electrons or muons with high transverse momenta. The data are consistent with the expected background from Standard Model processes. A statistical analysis leads to 95% confidence-level upper limits on the product of branching ratios $\mathcal{B}(t \to bH^{\pm}) \times \mathcal{B}(H^{\pm} \to \tau^{\pm}\nu)$, between 0.23% and 1.3% for charged Higgs boson masses in the range 80–160 GeV. It also leads to 95% confidence-level upper limits on the production cross section times branching ratio, $\sigma(pp \to tH^{\pm} + X) \times \mathcal{B}(H^{\pm} \to \tau^{\pm}\nu)$, between 0.76 pb and 4.5 fb, for charged Higgs boson masses ranging from 180 GeV to 1000 GeV. In the context of different scenarios of the Minimal Supersymmetric Standard Model, these results exclude nearly all values of $\tan\beta$ above one for charged Higgs boson masses between 80 GeV and 160 GeV, and exclude a region of parameter space with high $\tan\beta$ for $H^{\pm}$ masses between 200 GeV and 250 GeV.

Contents

1 Introduction **1**

2 Data and simulated events **3**

3 Physics object selection **5**

4 Event selection and background modelling **6**
- 4.1 Event selection 6
- 4.2 Data-driven estimation of the backgrounds with a true τ_{had} 7
- 4.3 Data-driven estimation of the multi-jet backgrounds 9
- 4.4 Backgrounds with electrons or muons misidentified as $\tau_{\text{had-vis}}$ 11
- 4.5 $\tau_{\text{had-vis}}$+$E_{\text{T}}^{\text{miss}}$ triggers 11
- 4.6 Event yields after the event selection 12

5 Systematic uncertainties **12**
- 5.1 $\tau_{\text{had-vis}}$+$E_{\text{T}}^{\text{miss}}$ triggers 12
- 5.2 Data-driven background estimation 13
- 5.3 Detector simulation 15
- 5.4 Generation of $t\bar{t}$ and signal events 16

6 Statistical analysis **16**

7 Results **18**

8 Conclusions **22**

9 Acknowledgements **22**

1 Introduction

Charged Higgs bosons (H^+, H^-) are predicted by several non-minimal Higgs scenarios, such as two-Higgs-doublet Models (2HDM) [1] or models containing Higgs triplets [2–6]. As the Standard Model (SM) does not contain any elementary charged scalar particle, the observation of a charged Higgs boson[1] would clearly indicate new phenomena beyond the SM. For instance, supersymmetric models predict the existence of charged Higgs bosons. In a type-II 2HDM, such as the Higgs sector of the Minimal Supersymmetric Standard Model (MSSM) [7–11], the main H^+ production mode at the Large Hadron Collider (LHC) would be through top-quark decays $t \to bH^+$, for charged Higgs boson masses (m_{H^+}) smaller than

[1] In the following, charged Higgs bosons are denoted by H^+, and the charge-conjugate is implied.

the top-quark mass (m_{top}). At the LHC, top quarks are produced predominantly through $t\bar{t}$ production. In this paper, the contribution to $t \to bH^+$ which may arise from single top-quark production is neglected, since the signal production cross section through this channel is very small with respect to $t\bar{t}$ production. A diagram illustrating the leading-order production mechanism is shown on the left-hand side of figure 1. For charged Higgs boson masses larger than m_{top}, the main H^+ source at the LHC is through associated production with a top quark. An additional b-quark can also appear in the final state. The leading-order production mechanisms in two different approximations are illustrated in the centre and right-hand side diagrams of figure 1: in the four-flavour scheme (4FS) b-quarks are dynamically produced, whereas in the five-flavour scheme (5FS) the b-quark is also considered as an active flavour inside the proton. Their cross sections are matched according to ref. [12], and an evaluation of the two schemes can be found in ref. [13].

In the MSSM, the Higgs sector can be completely determined at tree level by one of the Higgs boson masses, here taken to be m_{H^+}, and $\tan\beta$, the ratio of the vacuum expectation values of the two Higgs doublets. For $m_{H^+} < m_{\text{top}}$, the decay via $H^+ \to \tau^+\nu$ is dominant for $\tan\beta > 2$ and remains sizeable for $1 < \tan\beta < 2$. For higher m_{H^+}, the decay via $H^+ \to \tau^+\nu$ is still significant, especially for large values of $\tan\beta$ [14]. The combined LEP lower limit for the charged Higgs boson mass is about 90 GeV [15]. The Tevatron experiments placed upper limits on $\mathcal{B}(t \to bH^+)$ in the 15–20% range for $m_{\text{H}^+} < m_{\text{top}}$ [16, 17]. In a previous search based on data taken at $\sqrt{s} = 7$ TeV with the ATLAS and CMS detectors, the limits on $\mathcal{B}(t \to bH^+)$ were lowered to the range 0.8–4% [18, 19]. For all of these results, $\mathcal{B}(H^+ \to \tau^+\nu) = 100\%$ was assumed.

This paper describes a search for charged Higgs bosons with masses in the ranges 80–160 GeV and 180–1000 GeV. The region 160 GeV $< m_{H^+} <$ 180 GeV is not considered in this paper, since there is currently no reliable theoretical treatment for the interference between the different H^+ production modes in this transition region [20]. The final state studied is characterised by the presence of a hadronic τ decay (τ_{had}), missing transverse momentum ($E_{\text{T}}^{\text{miss}}$), b-quark-initiated jets, a hadronically decaying W boson, and the absence of any isolated electrons or muons with high transverse momenta. In addition to the large branching ratio for a τ to decay hadronically, this final state contains only neutrinos associated with the H^+ production and decay, resulting in good discriminating power between SM and signal processes. Charged Higgs bosons are searched for in a model-independent way, hence results are given in terms of $\mathcal{B}(t \to bH^+) \times \mathcal{B}(H^+ \to \tau^+\nu)$ (low-mass search, $m_{H^+} < m_{\text{top}}$) and $\sigma(pp \to \bar{t}H^+ + X) \times \mathcal{B}(H^+ \to \tau^+\nu)$ (high-mass search, $m_{H^+} > m_{\text{top}}$). These limits are then also interpreted in different MSSM scenarios. The results are based on 19.5 fb^{-1} of data from pp collisions at $\sqrt{s} = 8$ TeV, collected in 2012 with the ATLAS detector at the LHC. The final state analysed for the low-mass search is $t\bar{t} \to b\bar{b}W^-H^+ \to b\bar{b}(q\bar{q}')(\tau^+_{\text{had}}\nu)$. The final state is similar or identical for the high-mass search, depending on whether the additional b-quark-initiated jet is seen in the detector, $gb \to \bar{t}H^+ \to (W^-\bar{b})H^+ \to (q\bar{q}'\bar{b})(\tau^+_{\text{had}}\nu)$ in the 5FS case and $gg \to \bar{t}bH^+ \to (W^-\bar{b})bH^+ \to (q\bar{q}'\bar{b})b(\tau^+_{\text{had}}\nu)$ in the 4FS case.

This paper is organised as follows. In section 2, the data and simulated samples used

in this analysis are described. In section 3, the reconstruction of physics objects in ATLAS is discussed. The event selection and background modelling are presented in section 4. Systematic uncertainties are discussed in section 5, and the limit-setting procedure is described in section 6. Exclusion limits in terms of $\mathcal{B}(t \to bH^+) \times \mathcal{B}(H^+ \to \tau^+\nu)$ (low-mass) and $\sigma(pp \to \bar{t}H^+ + X) \times \mathcal{B}(H^+ \to \tau^+\nu)$ (high-mass) as well as model-dependent exclusion contours are presented in section 7.

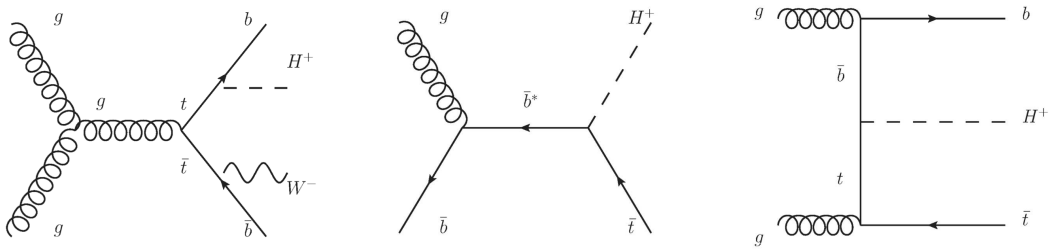

(a) low-mass H^+ production (b) 5FS high-mass H^+ production (c) 4FS high-mass H^+ production

Figure 1. Leading-order Feynman diagrams for the dominant production modes of charged Higgs bosons at masses (a) below and (b, c) above the top-quark mass.

2 Data and simulated events

The ATLAS detector [21] consists of an inner tracking detector with coverage in pseudorapidity[2] up to $|\eta| = 2.5$, surrounded by a thin 2 T superconducting solenoid, a calorimeter system extending up to $|\eta| = 4.9$ and a muon spectrometer extending up to $|\eta| = 2.7$ that measures the deflection of muon tracks in the field of three superconducting toroid magnets. A three-level trigger system is used. The first-level trigger (L1) is implemented in hardware, using a subset of detector information to reduce the event rate to no more than 75 kHz. This is followed by two software-based trigger levels (L2 and EF), which together further reduce the event rate to less than 1 kHz.

Only data taken with all ATLAS subsystems operational are used. Stringent detector and data quality requirements are applied, resulting in an integrated luminosity of 19.5 fb^{-1} for the 2012 data-taking period. The integrated luminosity has an uncertainty of 2.8%, measured following the methodology described in ref. [22]. Events are required to have a primary vertex with at least five associated tracks, each with a transverse momentum p_{T} greater than 400 MeV. The primary vertex is defined as the reconstructed vertex with the largest sum of squared track transverse momenta.

The background processes to this search include SM pair production of top quarks, as well as the production of single top-quark, W+jets, Z/γ^*+jets, diboson and multi-jet events. These backgrounds are categorised based on the type of reconstructed objects

[2] ATLAS uses a right-handed coordinate system with its origin at the nominal interaction point (IP) in the centre of the detector and the z-axis along the beam pipe. The x-axis points from the IP to the centre of the LHC ring, and the y-axis points upwards. Cylindrical coordinates (r, ϕ) are used in the transverse plane, ϕ being the azimuthal angle around the z-axis. The pseudorapidity is defined in terms of the polar angle θ as $\eta = -\ln\tan(\theta/2)$.

identified as the visible decay products [3] of the hadronically decaying τ candidate ($\tau_{\text{had-vis}}$). The dominant backgrounds in this analysis, those containing a true τ_{had}, where the $\tau_{\text{had-vis}}$ is correctly identified, or a jet misidentified as a $\tau_{\text{had-vis}}$ candidate, are estimated in a data-driven way (sections 4.2 and 4.3), while simulation samples are used to estimate the minor background arising from events with a lepton misidentified as a $\tau_{\text{had-vis}}$ (1–2% of the total background). Simulation samples are also used to develop and validate the analysis.

The modelling of SM $t\bar{t}$ and single top-quark events is performed with MC@NLO [23, 24], except for t-channel single top-quark production, for which AcerMC [25] is used. The top-quark mass is set to 172.5 GeV and the set of parton distribution functions used is CT10 [26]. For events generated with MC@NLO, the parton shower, hadronisation and underlying event are added using HERWIG [27] and JIMMY [28]. PYTHIA6 [29] is used instead for events generated with AcerMC. Inclusive cross sections are taken from the approximate next-to-next-to-leading-order (NNLO) predictions for $t\bar{t}$ production [30], for single top-quark production in the t-channel and s-channel [31, 32], as well as for Wt production [33]. Overlaps between SM Wt and $t\bar{t}$ final states are removed [24]. Single vector boson (W and Z/γ^*) production is simulated with up to five accompanying partons, using ALPGEN [34] interfaced to HERWIG and JIMMY, and using the CTEQ6L1 [35] parton distribution functions. The additional partons produced in the matrix-element part of the event generation can be light partons or heavy quarks. In the latter case, ALPGEN is also used to generate dedicated samples with matrix elements for the production of massive $b\bar{b}$ or $c\bar{c}$ pairs. Diboson events (WW, WZ and ZZ) are generated using HERWIG. The cross sections are normalised to NNLO predictions for W-boson and Z/γ^* production [36, 37] and to next-to-leading-order (NLO) predictions for diboson production [38]. The SM background samples are summarised in table 1.

Signal samples are produced with PYTHIA 6 for $80\,\text{GeV} \leq m_{H^+} \leq 160\,\text{GeV}$ in m_{H^+} intervals of 10 GeV separately for $t\bar{t} \to b\bar{b}H^+W^-$ and $t\bar{t} \to b\bar{b}H^-W^+$, where the charged Higgs bosons decay via $H^+ \to \tau^+\nu$. The process $t\bar{t} \to b\bar{b}H^+H^-$ gives a very small contribution to the signal region, which is negligible after the event selection described in section 4.1. The cross section for these processes depends only on the total $t\bar{t}$ production cross section and the branching ratio $\mathcal{B}(t \to bH^+)$. For $180\,\text{GeV} \leq m_{H^+} \leq 1000\,\text{GeV}$, the simulation of the signal for top-quark associated H^+ production is performed with POWHEG [39] interfaced to PYTHIA 8 [40]. For $180\,\text{GeV} \leq m_{H^+} \leq 200\,\text{GeV}$, samples are produced in m_{H^+} steps of 10 GeV, then in intervals of 25 GeV up to $m_{H^+} = 300\,\text{GeV}$ and in intervals of 50 GeV for $m_{H^+} \leq 600\,\text{GeV}$. Additionally, signal mass points at $m_{H^+} = 750\,\text{GeV}$ and $m_{H^+} = 1000\,\text{GeV}$ are produced. The production cross section for the high-mass charged Higgs boson is computed using the 4FS and 5FS, including theoretical uncertainties, and combined according to ref. [12]. The samples are generated at NLO using the 5FS and the narrow-width approximation for the H^+. Possible effects from the interference between the production of a charged Higgs boson through $t\bar{t}$ and top-quark associated production are not taken into account.

The event generators are tuned to describe the ATLAS data. In samples where

[3] This refers to the non-neutrino decay products.

Process	Generator	Cross section [pb]	
SM $t\bar{t}$ (inclusive)	MC@NLO	253	[30]
Single top-quark t-channel (≥ 1 lepton)	AcerMC	28.4	[31]
Single top-quark s-channel (≥ 1 lepton)	MC@NLO	1.8	[32]
Single top-quark Wt-channel (inclusive)	MC@NLO	22.4	[33]
$W \to \ell\nu$	ALPGEN	3.6×10^4	[36]
$Z/\gamma^* \to \ell\ell$ with $m(\ell\ell) > 10$ GeV	ALPGEN	1.7×10^4	[37]
WW (≥ 1 electron/muon)	HERWIG	20.9	[38]
ZZ (≥ 1 electron/muon)	HERWIG	1.5	[38]
WZ (≥ 1 electron/muon)	HERWIG	7.0	[38]
H^+ signal ($m_{H^+} = 250\,\text{GeV}$)	POWHEG	0.5	

Table 1. Cross sections for the simulated processes and reference generators used to model them. For the high-mass H^+ signal selection, the value shown is the cross section times $\mathcal{B}(H^+ \to \tau^+\nu)$ for the MSSM m_h^{max} scenario [41, 42], corresponding to $m_{H^+} = 250\,\text{GeV}$ and $\tan\beta = 50$. This cross section includes both H^+ and H^- production. The low-mass signal, which is not included in the table, assumes one H^+ produced per $t\bar{t}$ decay, so it is a fraction of the $t\bar{t}$ cross section. The previously published upper limit on $\mathcal{B}(t \to bH^+)$ for $m_{H^+} = 130\,\text{GeV}$ is 0.9% [18].

PYTHIA 6 is interfaced to AcerMC, the AUET2B [43] tune is used. The Perugia 2011 C tune [44] is used when PYTHIA 6 is interfaced to POWHEG. For the samples generated with HERWIG, the AUET2 [45] tune is used. In all samples with τ leptons, except for those simulated with PYTHIA 8[4], TAUOLA [46] is used for the τ decays. PHOTOS [47] is used for photon radiation from charged leptons in all samples where applicable.

To take into account the presence of multiple proton–proton interactions occurring in the same and neighbouring bunch crossings (referred to as pile-up), simulated minimum-bias events are added to the hard process in each generated event. Prior to the analysis, simulated events are reweighted in order to match the distribution of the average number of pile-up interactions in the data. All generated events are propagated through a detailed GEANT4 simulation [48, 49] of the ATLAS detector and are reconstructed with the same algorithms as the data.

3 Physics object selection

Jets are reconstructed from energy deposits in the calorimeters, using the anti-k_t algorithm [50, 51] with a radius parameter of $R = 0.4$. Jets are required to have $p_{\text{T}} > 25\,\text{GeV}$ and $|\eta| < 2.5$. To reduce the contribution of jets initiated by pile-up, jets with $p_{\text{T}} < 50\,\text{GeV}$ and $|\eta| < 2.4$ must pass the requirement that at least half of the p_{T} of the tracks associated with the jet is contributed by tracks matched to the primary vertex [52]. An algorithm identifies jets containing b-quarks by combining impact parameter information with the explicit determination of a secondary vertex [53], and these are referred to as b-tagged jets.

[4]So-called "sophisticated tau-decays" have been available in PYTHIA since version 8.150 such that the usage of TAUOLA is not necessary.

A working point corresponding to a 70% efficiency for identifying b-quark-initiated jets is used.

Candidates for identification as $\tau_{\text{had-vis}}$ arise from jets reconstructed from energy deposits in calorimeters, again using the anti-k_t algorithm with a radius parameter of $R = 0.4$, which have $p_{\text{T}} > 10\,\text{GeV}$ and one or three charged-particle tracks within a cone of size of $\Delta R < 0.2$, where $\Delta R = \sqrt{(\Delta\eta)^2 + (\Delta\phi)^2}$ around the $\tau_{\text{had-vis}}$ axis [54]. These candidates are further required to have a visible transverse momentum (p_{T}^{τ}) of at least 20 GeV and to be within $|\eta| < 2.3$. The output of boosted decision tree algorithms [55, 56] is used to distinguish $\tau_{\text{had-vis}}$ from jets not initiated by τ leptons, separately for τ_{had} decays with one or three charged-particle tracks. In this analysis, a point with 40% (35%) efficiency for identification of 1(3)-prong $\tau_{\text{had-vis}}$ is used, and this requirement is referred to as the $\tau_{\text{had-vis}}$ identification. Dedicated algorithms are used to reject electrons and muons that are incorrectly identified as $\tau_{\text{had-vis}}$ [54]. After these algorithms are applied, the backgrounds arising from muons and electrons misidentified as $\tau_{\text{had-vis}}$ are very small, although there is still a sizeable background from jets misidentified as $\tau_{\text{had-vis}}$.

The $E_{\text{T}}^{\text{miss}}$ is defined as the magnitude of the negative vectorial sum of transverse momenta of muons and energy deposits in the calorimeter. It is computed using fully calibrated and reconstructed physics objects [57].

The final states considered in this search contain no charged leptons, hence events containing isolated electron or muon candidates with high transverse momenta are rejected. Electron candidates are reconstructed from energy deposits in the calorimeter that are matched to tracks in the inner detector, taking losses due to bremsstrahlung into account. They are required to have a transverse energy (E_{T}) greater than 25 GeV and to be within $|\eta| < 2.47$ (the transition region between the barrel and end-cap calorimeters, $1.37 < |\eta| < 1.52$, is excluded) [58, 59]. Muon candidates must pass tracking requirements in both the inner detector and the muon spectrometer, have $p_{\text{T}} > 25\,\text{GeV}$ and $|\eta| < 2.5$ [60]. Additionally, electron candidates are required to pass pile-up-corrected 90% efficient calorimeter- and track-based isolation, with ΔR cone sizes of 0.2 and 0.3, respectively, while muon candidates are required to pass a relative track-based isolation of < 0.05 with a ΔR cone < 0.4 [61].

4 Event selection and background modelling

4.1 Event selection

The analysis uses events passing a $\tau_{\text{had-vis}}$+$E_{\text{T}}^{\text{miss}}$ trigger. The $\tau_{\text{had-vis}}$ trigger is defined by calorimeter energy in a narrow core region and an isolation region at L1, a basic combination of tracking and calorimeter information at L2 and more sophisticated algorithms imported from the offline reconstruction at the EF. The $E_{\text{T}}^{\text{miss}}$ trigger uses calorimeter information at all levels with a more refined algorithm at the EF. The EF threshold on the transverse momentum of the $\tau_{\text{had-vis}}$ trigger object is 27 GeV or 29 GeV, and for the $E_{\text{T}}^{\text{miss}}$ trigger the EF threshold is 40 GeV or 50 GeV. The multiple trigger thresholds are the result of slight changes of the trigger definition during the 2012 data-taking period, for which 50%

of events had EF thresholds at 27 GeV and 50 GeV, 43% at 29 GeV and 50 GeV, and 7% at 29 GeV and 40 GeV, for the $\tau_{\text{had-vis}}$ and $E_{\text{T}}^{\text{miss}}$ triggers, respectively.

Further event filtering is performed by discarding events in which any jet with $p_{\text{T}} > 25$ GeV fails the quality cuts discussed in ref. [62]. This ensures that no jet is consistent with having originated from instrumental effects or non-collision backgrounds. The following requirements are then applied:

- at least four (three) selected jets for the low-mass (high-mass) signal selection;
- at least one of these selected jets being b-tagged at the 70%-efficient working point;
- exactly one selected $\tau_{\text{had-vis}}$ with $p_{\text{T}}^{\tau} > 40$ GeV matched to a $\tau_{\text{had-vis}}$ trigger object (trigger-matched);
- no selected electron or muon in the event;
- $E_{\text{T}}^{\text{miss}} > 65$ (80) GeV for the low-mass (high-mass) signal selection;
- $E_{\text{T}}^{\text{miss}}/\sqrt{\sum p_{\text{T}}^{\text{PV trk}}} > 6.5$ (6.0) GeV$^{1/2}$ for the low-mass (high-mass) signal selection, where $\sum p_{\text{T}}^{\text{PV trk}}$ is the sum of transverse momenta of all tracks originating from the primary vertex. This is to reject events in which a large reconstructed $E_{\text{T}}^{\text{miss}}$ is due to the limited resolution of the energy measurement.

For the selected events, the transverse mass (m_{T}) of the $\tau_{\text{had-vis}}$ and $E_{\text{T}}^{\text{miss}}$ is defined as:

$$m_{\text{T}} = \sqrt{2 p_{\text{T}}^{\tau} E_{\text{T}}^{\text{miss}} (1 - \cos \Delta\phi_{\tau,\text{miss}})}, \tag{4.1}$$

where $\Delta\phi_{\tau,\text{miss}}$ is the azimuthal angle between the $\tau_{\text{had-vis}}$ and the direction of the missing transverse momentum. This discriminating variable takes values lower than the W boson mass for $W \to \tau\nu$ background events and less than the H^+ mass for signal events, in the absence of detector resolution effects.

A minimal requirement is placed on m_{T} at 20 (40) GeV in the low-mass (high-mass) H^+ search. This requirement is motivated in section 4.2. After the full event selection, the signal has an acceptance of 0.30–0.60% for the low-mass range, and 1.7–5.8% for the high-mass range, where in both cases the acceptance increases with increasing m_{H^+}. The acceptances are evaluated with respect to signal samples where both the τ lepton and the associated top quark decay inclusively.

4.2 Data-driven estimation of the backgrounds with a true τ_{had}

An embedding method [63] is used to estimate the backgrounds that contain a real τ_{had} from a vector boson decay. The method is based on a control data sample of μ+jets events satisfying criteria similar to those of the signal selection except for the $\tau_{\text{had-vis}}$ requirements and replacing the detector signature of the muon by a simulated hadronic τ decay. The method is applied to a control region of μ+jets events, rather than e+jets, due to the clean signature and the relative ease with which the measured muon can be removed. These new hybrid events are then used for the background prediction. An advantage of this approach,

compared to simulation, is that with the exception of the τ_{had}, the estimate is extracted from data; this includes the contributions from the underlying event and pile-up, jets, and all sources of $E_{\text{T}}^{\text{miss}}$ except for the neutrino from the τ_{had} decay. Furthermore, since the normalisation of the background estimate is evaluated from the data, assuming lepton universality of the W boson decay, the method does not rely on theoretical cross sections and their uncertainties. This embedding method has been used in previous charged Higgs boson searches [64] as well as in SM $H \to \tau\tau$ [65, 66] analyses.

To select the μ+jets sample from the data, the following requirements are made:

- a single-muon trigger with a p_{T} threshold of 24 GeV or 36 GeV (single-muon triggers with two different p_{T} thresholds are used, since the lower-threshold trigger also requires the muon to be isolated);
- exactly one isolated muon with $p_{\text{T}} > 25$ GeV and no isolated electron with $E_{\text{T}} > 25$ GeV;
- at least four (three) jets with $p_{\text{T}} > 25$ GeV for the low-mass (high-mass) charged Higgs boson search, at least one of which is b-tagged;
- $E_{\text{T}}^{\text{miss}} > 25$ (40) GeV for the low-mass (high-mass) charged Higgs boson search.

This selection is looser than the selection defined in section 4.1 in order not to bias the sample. However, the $E_{\text{T}}^{\text{miss}}$ cut in the μ+jets sample selection removes events with very low m_{T}. Thus, a cut on $m_{\text{T}} > 20$ (40) GeV is introduced in the search for low-mass (high-mass) charged Higgs bosons to remove this bias. With this selection, there is a possible small contamination from signal events with a leptonically decaying τ lepton. This small contamination, which is estimated using simulation, has a much softer m_{T} distribution than the signal with τ_{had}, and is observed to have a negligible impact on the evaluation of signal strength or exclusion limits. Contamination from leptonically decaying τ leptons from W decays is accounted for in the overall normalisation ($c_{\tau\to\mu}$ in eq. (4.3)).

To replace a muon in the selected data, the track that is associated with the muon is removed. The energy deposited in the calorimeters is removed by simulating a $W \to \mu\nu$ event with the same kinematics as in the selected data event and identifying the corresponding cells. Thus, the removal of energy deposits not associated with the selected muon is minimised. The momentum of the muon in selected events is extracted and rescaled to account for the higher τ lepton mass,

$$\vec{p}_{\tau} = \frac{\sqrt{E_{\mu}^2 - m_{\tau}^2}}{\sqrt{\vec{p}_{\mu} \cdot \vec{p}_{\mu}}} \vec{p}_{\mu}, \tag{4.2}$$

where $\vec{p}_{\tau}$ is the rescaled momentum, E_{μ} is the reconstructed energy of the muon, m_{τ} is the τ mass, and $\vec{p}_{\mu}$ is the reconstructed muon momentum. The τ lepton with rescaled momentum is further processed by TAUOLA to produce the hadronic τ decay and account for the τ polarisation as well as for final-state radiation. The τ lepton decay products are propagated through the full detector simulation and reconstruction. Events referred to

as containing a true τ_{had} are those with a genuine τ_{had} as expected from the embedding method.

The shape of the m_{T} distributions for backgrounds with a true τ_{had} is taken from the distribution obtained with the embedded events, after applying the corresponding signal selection. The normalisation is then derived from the number of embedded events:

$$N_\tau = N_{\text{embedded}} \cdot (1 - c_{\tau\to\mu}) \frac{\epsilon^{\tau+E_{\text{T}}^{\text{miss}}-\text{trigger}}}{\epsilon^{\mu-\text{ID,trigger}}} \times \mathcal{B}(\tau \to \text{hadrons} + \nu), \tag{4.3}$$

where N_τ is the estimated number of events with a true τ_{had}, N_{embedded} is the number of embedded events in the signal region, $c_{\tau\to\mu}$ is the fraction of events in which the selected muon is a decay product of a τ lepton (taken from simulation, about 4%), $\epsilon^{\tau+E_{\text{T}}^{\text{miss}}-\text{trigger}}$ is the $\tau_{\text{had-vis}}+E_{\text{T}}^{\text{miss}}$ trigger efficiency (as a function of p_{T}^{τ} and $E_{\text{T}}^{\text{miss}}$, derived from data, see section 4.5), $\epsilon^{\mu-\text{ID,trigger}}$ is the muon trigger and identification efficiency (as a function of p_T and η, derived from data) and $\mathcal{B}(\tau \to \text{hadrons} + \nu)$ is the branching ratio of the τ lepton decays to hadrons.

The m_{T} distributions for selected events with a true τ_{had}, as obtained with the embedding method, are shown in figure 2 and compared to simulation. Embedded data and simulation agree well and are within uncertainties. The combined systematic and statistical uncertainties on the embedded prediction and simulation are compared directly in figure 2, where the reduction provided by the use of the embedding method is shown.

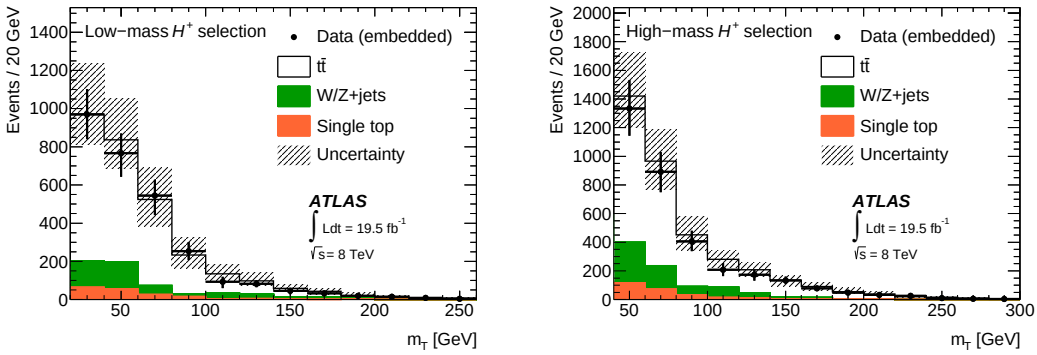

(a) Low-mass H^+ selection

(b) High-mass H^+ selection

Figure 2. Comparison of the m_{T} distributions for events with a true τ_{had} for the (a) low-mass and (b) high-mass charged Higgs boson search, as predicted by the embedding method and simulation. Combined statistical and systematic uncertainties (as described in section 5) for the embedded sample are shown as error bars, and all systematic uncertainties applicable to simulation are shown as hatched bands.

4.3 Data-driven estimation of the multi-jet backgrounds

For the data-driven estimation of the backgrounds with a jet misidentified as a $\tau_{\text{had-vis}}$ (multi-jet background), two data samples are defined, differing only in $\tau_{\text{had-vis}}$ identification criteria. The *tight* sample contains a larger fraction of events with a real $\tau_{\text{had-vis}}$, which are

required to pass the *tight* $\tau_{\text{had-vis}}$ identification selection described in the object selection, in addition to the trigger matching required in the event selection of section 4.1. The *loose* sample, which contains a larger fraction of events with a misidentified $\tau_{\text{had-vis}}$, is obtained by removing the $\tau_{\text{had-vis}}$ identification requirement that was applied in the *tight* sample. By construction, the *tight* data sample is a subset of the *loose* data sample.

The *loose* sample consists of N_{r} and N_{m} events with, respectively, a real or misidentified $\tau_{\text{had-vis}}$. It is also composed of N_{L} events with a $\tau_{\text{had-vis}}$ passing a *loose but not tight* selection, and N_{T} events in which the $\tau_{\text{had-vis}}$ fulfils the *tight* selection. Using the efficiencies p_{r} and p_{m}, respectively, for a real or misidentified *loose* $\tau_{\text{had-vis}}$ satisfying the *tight* criteria, the following relation can be established:

$$\begin{pmatrix} N_{\text{T}} \\ N_{\text{L}} \end{pmatrix} = \begin{pmatrix} p_{\text{r}} & p_{\text{m}} \\ (1-p_{\text{r}}) & (1-p_{\text{m}}) \end{pmatrix} \times \begin{pmatrix} N_{\text{r}} \\ N_{\text{m}} \end{pmatrix}. \tag{4.4}$$

In turn, inverting the 2×2 matrix above, the number of events in which the misidentified $\tau_{\text{had-vis}}$ passes the *tight* selection can be written as:

$$N_{\text{m}}^{\text{T}} = p_{\text{m}} N_{\text{m}} = \frac{p_{\text{m}} p_{\text{r}}}{p_{\text{r}} - p_{\text{m}}} N_{\text{L}} + \frac{p_{\text{m}}(p_{\text{r}} - 1)}{p_{\text{r}} - p_{\text{m}}} N_{\text{T}}. \tag{4.5}$$

The final values of p_{r} and p_{m} are parameterised in terms of the number of charged-particle tracks in the core cone ($\Delta R \leq 0.2$) and the number of charged-particle tracks in the hollow isolation cone ($0.2 < \Delta R < 0.4$) around the $\tau_{\text{had-vis}}$ axis [54], as well as the p_{T} and $|\eta|$ of the $\tau_{\text{had-vis}}$. Correlations between the variables used for parameterisation are found to have a negligible effect on the results of the method.

The probability p_{r} is determined using true $\tau_{\text{had-vis}}$ in simulated $t\bar{t}$ events in the signal region. The probability p_{m} is measured in a W+jets control region in data. Events in this control region are triggered by a combined trigger requiring an electron with $E_{\text{T}} > 18\,\text{GeV}$ or a muon with $p_{\text{T}} > 15\,\text{GeV}$ in addition to a $\tau_{\text{had-vis}}$. In both cases, the $\tau_{\text{had-vis}}$ trigger object has a p_{T} threshold of 20 GeV. The control region must have exactly one trigger-matched reconstructed electron or muon, in addition to a trigger-matched, reconstructed, *loose* $\tau_{\text{had-vis}}$. The control region is also required to have zero b-tagged jets and $m_{\text{T}}(e/\mu, E_{\text{T}}^{\text{miss}}) > 50\,\text{GeV}$ (using eq.(4.1), with the $\tau_{\text{had-vis}}$ replaced by the electron or muon). The contamination from correctly reconstructed $\tau_{\text{had-vis}}$ (7%) and electrons or muons mis-reconstructed as $\tau_{\text{had-vis}}$ (5%) is subtracted using simulation. Signal processes contribute negligibly to this region ($< 0.1\%$).

Having computed the identification and misidentification efficiencies p_{r} and p_{m}, every event in the *loose* sample is given a weight w as follows, in order to estimate the background with a misidentified $\tau_{\text{had-vis}}$ in the *tight* sample:

- for an event with a *loose but not tight* $\tau_{\text{had-vis}}$, $w_{\text{L}} = \dfrac{p_{\text{m}} p_{\text{r}}}{p_{\text{r}} - p_{\text{m}}}$;
- for an event with a *tight* $\tau_{\text{had-vis}}$, $w_{\text{T}} = \dfrac{p_{\text{m}}(p_{\text{r}} - 1)}{p_{\text{r}} - p_{\text{m}}}$.

Events with jets misidentified as $\tau_{\text{had-vis}}$ are a major background in the high-m_{T} region ($> 300\,\text{GeV}$ low-mass and $> 400\,\text{GeV}$ high-mass), but this region has less than one expected

event per 20 GeV bin. This limitation is circumvented by fitting the m_{T} distribution using a power-log function in the mass range 200–800 GeV. The power-log function is defined by the following formula:

$$f(x) = x^{a+b\ln(x)}, \tag{4.6}$$

where a and b are fitted constants. The resulting m_{T} distribution after considering each systematic uncertainty is fitted separately. An additional systematic uncertainty is added for the choice of fit function, by symmetrising the difference between the baseline fit and an alternative fit using an exponential function. The exponential is chosen to probe the effect on the expected yield in the poor statistics tail region, since it also describes the multi-jet background well in the region with many events. Figure 3 shows the fits obtained in the nominal case, for the systematic uncertainty due to the chosen fit function, and for all other systematic uncertainties related to this background estimation (see section 5.2).

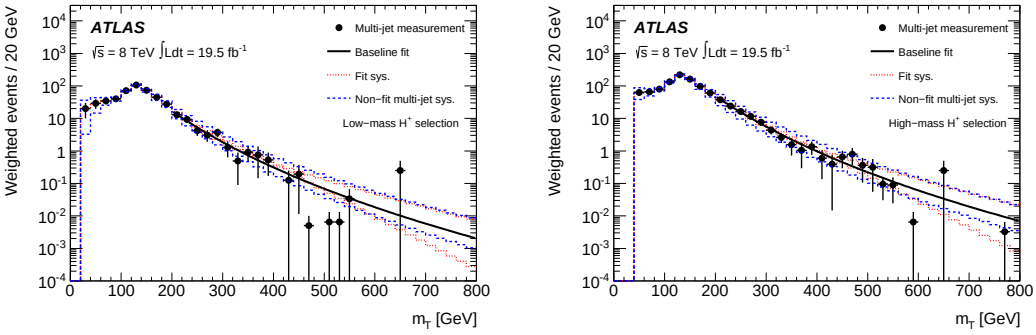

(a) Low-mass H^+ selection

(b) High-mass H^+ selection

Figure 3. The multi-jet background predictions from data-driven methods for the (a) low-mass and (b) high-mass H^+ event selections, with the results of fits using the power-log function, are shown in the solid line. The dotted lines show the systematic uncertainty from the choice of the fit function. The dashed lines show the total combined fits from the sources of systematic uncertainty listed in table 4.

4.4 Backgrounds with electrons or muons misidentified as $\tau_{\text{had-vis}}$

Backgrounds that arise from events where an electron or muon is misidentified as $\tau_{\text{had-vis}}$ are heavily suppressed by dedicated veto algorithms, so that these events only contribute at the level of 1–2% to the total background. These backgrounds are estimated from simulated events, and they include contributions from $t\bar{t}$, single top-quark, diboson, W+jets and Z+jets processes. Leptons from in-flight decays in multi-jet events are accounted for in the multi-jet background estimate.

4.5 $\tau_{\text{had-vis}}+E_{\mathrm{T}}^{\text{miss}}$ triggers

The analysis presented in this paper relies on $\tau_{\text{had-vis}}+E_{\mathrm{T}}^{\text{miss}}$ triggers. To correct for any difference between the trigger efficiencies observed in simulation and those observed in data, p_{T}^{τ}- and $E_{\mathrm{T}}^{\text{miss}}$-dependent correction factors are derived, whose evaluation is limited

by statistical uncertainties. To increase the sample size, the $\tau_{\text{had-vis}}$ and $E_{\text{T}}^{\text{miss}}$ trigger efficiencies are determined separately and residual effects due to correlations are taken into account as systematic uncertainties. To measure the efficiencies, a tag-and-probe method is used in a control region enriched with $t\bar{t}$ events with a $\mu+\tau_{\text{had}}$ selection using a muon trigger with a p_{T} threshold of 24 GeV or 36 GeV. The trigger efficiencies are fitted separately for events with a $\tau_{\text{had-vis}}$ that has one or three charged-particle tracks. The p_{T}^{τ} ($E_{\text{T}}^{\text{miss}}$) trigger efficiencies are fitted in the range of 20–100 (20–500) GeV. The ratios of the fitted functions for data and simulation are then applied to the simulated samples as continuous correction factors.

Since no trigger information is available in the embedded sample, trigger efficiencies are applied to that sample. The efficiencies for the $\tau_{\text{had-vis}}$ trigger derived as described above need to be corrected for misidentified $\tau_{\text{had-vis}}$. The fraction of events with a misidentified $\tau_{\text{had-vis}}$ is substantial in the $\mu + \tau_{\text{had}}$ sample used for the tag-and-probe method, leading to a lower efficiency than in a sample with only events that have a true $\tau_{\text{had-vis}}$. Since only events with a true $\tau_{\text{had-vis}}$ are present in the embedded sample, the efficiencies determined from data are corrected by the ratio of the simulated efficiency for true $\tau_{\text{had-vis}}$ to the simulated efficiency for the $\mu + \tau_{\text{had}}$ sample.

4.6 Event yields after the event selection

The expected numbers of background events and the results from data, together with an expectation from signal contributions in the low-mass and high-mass H^+ selections, are shown in table 2. For the low-mass H^+ search, the signal contribution is shown for a cross section corresponding to $\mathcal{B}(t \to bH^+) \times \mathcal{B}(H^+ \to \tau\nu) = 0.9\%$, and for the high-mass H^+ search a possible signal contribution in the m_h^{max} scenario of the MSSM with $\tan\beta = 50$ is shown.

The number of events with a true τ_{had} is derived from the number of embedded events and does not depend on the theoretical cross section of the $t\bar{t} \to b\bar{b}W^+W^-$ process. However, this analysis does rely on the theoretical inclusive $t\bar{t}$ production cross section $\sigma_{t\bar{t}} = 253^{+13}_{-15}$ pb [30] for the estimation of the small background with electrons or muons misidentified as $\tau_{\text{had-vis}}$.

5 Systematic uncertainties

5.1 $\tau_{\text{had-vis}}$+$E_{\text{T}}^{\text{miss}}$ triggers

Systematic uncertainties on the measurement of the $\tau_{\text{had-vis}}$+$E_{\text{T}}^{\text{miss}}$ trigger efficiencies arise from multiple sources: the selection of the muon in the μ+τ_{had} sample, the number of misidentified $\tau_{\text{had-vis}}$, the choice of fitting function, slightly varying trigger requirements during the data-taking period, a residual correlation between the $\tau_{\text{had-vis}}$ and $E_{\text{T}}^{\text{miss}}$ triggers, and the effect of the $\tau_{\text{had-vis}}$ energy correction on the trigger efficiency. The dominant systematic uncertainty, which arises from misidentified $\tau_{\text{had-vis}}$ in the $t\bar{t} \to \mu\tau_{\text{had}} + X$ control region, is evaluated by measuring the trigger correction factors after varying the expected misidentified $\tau_{\text{had-vis}}$ yield by its uncertainty. These uncertainties are relevant

Sample	Low-mass H^+ selection	High-mass H^+ selection
True τ_{had} (embedding method)	$2800 \pm 60 \pm 500$	$3400 \pm 60 \pm 400$
Misidentified jet $\to \tau_{\text{had-vis}}$	$490 \pm 9 \pm 80$	$990 \pm 15 \pm 160$
Misidentified $e \to \tau_{\text{had-vis}}$	$15 \pm 3 \pm 6$	$20 \pm 2 \pm 9$
Misidentified $\mu \to \tau_{\text{had-vis}}$	$18 \pm 3 \pm 8$	$37 \pm 5 \pm 8$
All SM backgrounds	$3300 \pm 60 \pm 500$	$4400 \pm 70 \pm 500$
Data	3244	4474
H^+ ($m_{H^+} = 130\,\text{GeV}$)	$230 \pm 10 \pm 40$	
H^+ ($m_{H^+} = 250\,\text{GeV}$)		$58 \pm 1 \pm 9$

Table 2. Expected event yields after all selection criteria and comparison with $19.5\,\text{fb}^{-1}$ of data. The values shown for the signal correspond to the previously published upper limit on $\mathcal{B}(t \to bH^+) \times \mathcal{B}(H^+ \to \tau\nu) = 0.9\%$ [18] for the low-mass signal point and $\tan\beta = 50$ in the MSSM m_h^{max} scenario for the high-mass signal point. The predicted yield for the low-mass signal selection assumes a $t\bar{t}$ cross section of 253 pb. Both the statistical and systematic uncertainties (section 5) are shown, in this order.

Source of uncertainty	Low-mass H^+ selection	High-mass H^+ selection
Muon selection	$< 1\%$	$< 1\%$
Misidentified $\tau_{\text{had-vis}}$	5.6%	5.7%
Fitting function	2.1%	1.8%
Trigger definition	$< 1\%$	$< 1\%$
Residual correlations	1.4%	3.2%
$\tau_{\text{had-vis}}$ energy scale	$< 1\%$	$< 1\%$

Table 3. Effect of systematic uncertainties on the combined trigger efficiencies for a low-mass ($m_{H^+} = 130\,\text{GeV}$) and high-mass ($m_{H^+} = 250\,\text{GeV}$) signal sample.

for background events with leptons misidentified as $\tau_{\text{had-vis}}$ as well as true τ_{had} and signal events. The effects on a low-mass and a high-mass signal sample are summarised in table 3 and the effect on background events with true τ_{had} is shown in table 4. The trigger correction factors used to account for differences between the efficiencies in simulation and data are shown in figure 4.

5.2 Data-driven background estimation

The systematic uncertainties arising from the data-driven methods used to estimate the various backgrounds are summarised in table 4.

The systematic uncertainties affecting the estimation of the backgrounds with true τ_{had}, discussed in section 4.2, consist of the potential bias introduced by the embedding method itself (embedding parameters, evaluated by varying the amount of energy that is subtracted when removing calorimeter deposits of the muon in the original event), uncer-

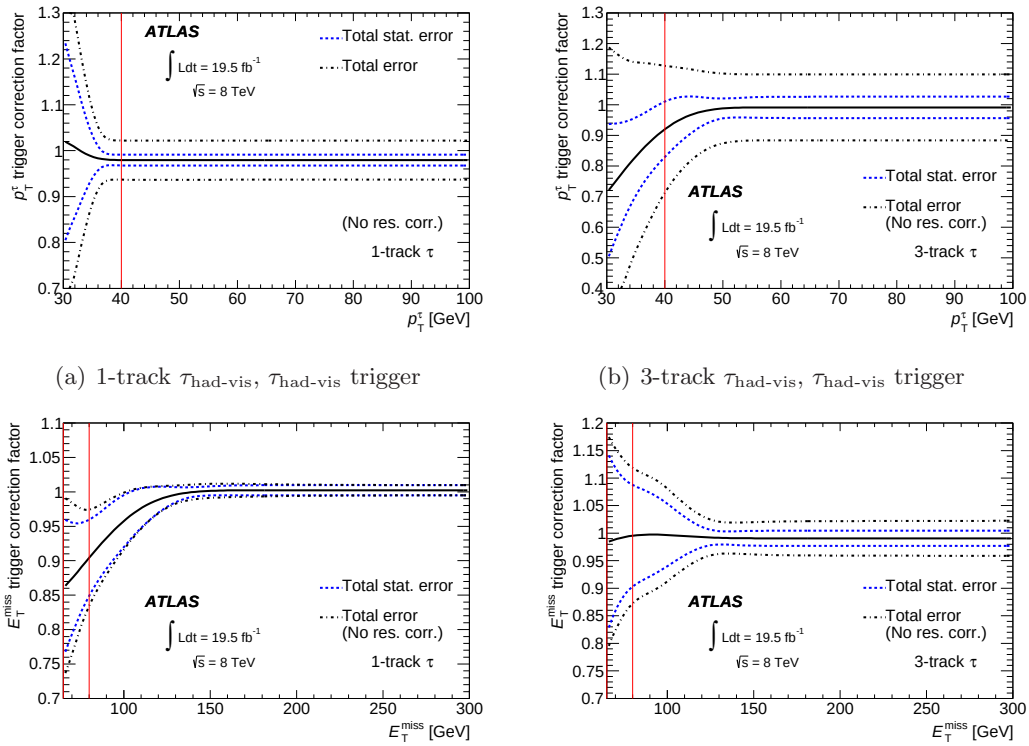

(a) 1-track $\tau_{\text{had-vis}}$, $\tau_{\text{had-vis}}$ trigger

(b) 3-track $\tau_{\text{had-vis}}$, $\tau_{\text{had-vis}}$ trigger

(c) 1-track $\tau_{\text{had-vis}}$, $E_{\text{T}}^{\text{miss}}$ trigger

(d) 3-track $\tau_{\text{had-vis}}$, $E_{\text{T}}^{\text{miss}}$ trigger

Figure 4. Inclusive $\tau_{\text{had-vis}}$ and $E_{\text{T}}^{\text{miss}}$ trigger correction factors obtained from the ratio of functions fitted to data and simulation for $\tau_{\text{had-vis}}$ with (a, c) one and (b, d) three charged tracks are shown at the top and bottom, respectively. The vertical line on the $\tau_{\text{had-vis}}$ trigger correction factor plots indicates the lowest p_{T}^{τ} threshold used in the analysis. The vertical line on the $E_{\text{T}}^{\text{miss}}$ trigger correction factor plots shows the lower boundary used in the high-mass charged Higgs boson search. The total statistical uncertainty is indicated with the dotted line and the systematic uncertainty is added in quadrature to the statistical error (dashed-dotted line). For $\tau_{\text{had-vis}}$ trigger efficiencies, the total systematic uncertainty is shown, while for the $E_{\text{T}}^{\text{miss}}$ trigger efficiency, the systematic uncertainty related to residual correlations between $\tau_{\text{had-vis}}$ and $E_{\text{T}}^{\text{miss}}$ is not included, since the effect is evaluated separately for several signal mass ranges and background samples.

tainties from the trigger efficiency measurement as discussed in section 5.1, uncertainties due to a possible contamination from multi-jet events (evaluated by varying the muon isolation requirements), uncertainties associated with the simulated τ_{had} ($\tau_{\text{had-vis}}$ energy scale and identification efficiency) and uncertainties on the normalisation. The latter are dominated by the statistical uncertainty of the selected control sample and the $\tau_{\text{had-vis}}$+$E_{\text{T}}^{\text{miss}}$ trigger efficiency uncertainties.

For the estimation of backgrounds with jets misidentified as $\tau_{\text{had-vis}}$, discussed in section 4.3, the dominant systematic uncertainties on the misidentification probability are the statistical uncertainty due to the control sample size and uncertainties due to the difference in the jet composition (gluon- or quark-initiated) between the control and signal regions. The uncertainty arising from differences in jet composition is evaluated from the difference

Source of uncertainty	Low-mass H^+ selection	High-mass H^+ selection
True τ_{had}		
Embedding parameters	3.0%	1.8%
Muon isolation	0.3%	2.3%
Parameters in normalisation	2.0%	2.0%
$\tau_{\text{had-vis}}$ identification	2.2%	2.0%
$\tau_{\text{had-vis}}$ energy scale	4.0%	3.6%
$\tau_{\text{had-vis}} + E_{\text{T}}^{\text{miss}}$ trigger	8.3%	8.3%
Jet $\rightarrow \tau_{\text{had-vis}}$		
Statistical uncertainty on p_{m}	2.0%	3.4%
Statistical uncertainty on p_{r}	0.5%	0.5%
Jet composition	1.1%	1.9%
$\tau_{\text{had-vis}}$ identification	0.8%	0.6%
e/μ contamination	0.5%	0.7%

Table 4. Dominant systematic uncertainties on the data-driven background estimates. The shift in event yield is given relative to the total background.

in shape and normalisation that arises when p_{m} is measured in a control region that is enriched in events with gluon-initiated jets. This control region differs from the signal region only by inverting the b-tag and $E_{\text{T}}^{\text{miss}}$ requirements. Other uncertainties are due to the statistical uncertainty on p_{r}, the effect of the uncertainty in the simulated true $\tau_{\text{had-vis}}$ identification efficiency on the measurement of p_{r} and p_{m}, and the effect of the simulated electron veto efficiency for true electrons on the measurement of p_{m}.

5.3 Detector simulation

Systematic uncertainties originating from the simulation of pile-up and object reconstruction are considered for signal events and background events with leptons misidentified as $\tau_{\text{had-vis}}$. This background is roughly 1% of the final background in both the low-mass and high-mass searches, so the systematic uncertainties have little effect on the final results.

Uncertainties related to the $\tau_{\text{had-vis}}$ energy scale and identification efficiency are also taken into account. The uncertainty on the identification is in the range 2−3% for $\tau_{\text{had-vis}}$ with one charged track and 3−5% for $\tau_{\text{had-vis}}$ with three charged tracks. It has been measured in data using a tag-and-probe method [54]. The $\tau_{\text{had-vis}}$ energy scale is measured with a precision of 2−4% [67]. It is determined by fitting the reconstructed visible mass of $Z \rightarrow \tau\tau$ events in data. Uncertainties related to jet or b-tagged jet energy scale, energy resolution, flavour identification and calibration, and the effects of pile-up interactions are also taken into account [68, 69], as well as uncertainties related to the reconstruction of $E_{\text{T}}^{\text{miss}}$ [70].

The impact of most sources of systematic uncertainty is assessed by re-applying the selection cuts for each analysis after varying a particular parameter by its ±1 standard deviation uncertainty. The dominant instrumental systematic uncertainties include the jet

energy scale, the $\tau_{\text{had-vis}}$ energy scale, and $\tau_{\text{had-vis}}$ identification. All instrumental systematic uncertainties are taken into account for the reconstruction of $E_{\text{T}}^{\text{miss}}$.

These uncertainties affect all simulated samples, i.e. the signal and the background contribution with leptons misidentified as $\tau_{\text{had-vis}}$. Since the τ_{had} in the embedded samples are simulated, all τ_{had}-related uncertainties are relevant for the background with true τ_{had} as well.

5.4 Generation of $t\bar{t}$ and signal events

In order to estimate the systematic uncertainties arising from the $t\bar{t}$ and low-mass signal generation, as well as from the parton shower model, the acceptance is computed for $t\bar{t}$ events produced with MC@NLO interfaced to HERWIG/JIMMY and POWHEG interfaced to PYTHIA 8. Also, an uncertainty on the theoretical cross section, including both the factorisation/renormalisation scale and parton distribution function uncertainties, is taken into account for $t\bar{t}$ backgrounds with a lepton misidentified as a $\tau_{\text{had-vis}}$ and low-mass signal samples. The estimate of the small background with electrons or muons misidentified as $\tau_{\text{had-vis}}$ relies additionally on the theoretical inclusive $t\bar{t}$ production cross section $\sigma_{t\bar{t}} = 253^{+13}_{-15}$ pb [30].

The generator modelling uncertainties for the high-mass signal samples are estimated from a comparison between events produced with MC@NLO interfaced to HERWIG++ [71] and POWHEG interfaced to PYTHIA 8.

The systematic uncertainties originating from initial- and final-state parton radiation, which modify the jet production rate, are computed for $t\bar{t}$ backgrounds and applied to low-mass signal events by using $t\bar{t}$ samples generated with AcerMC interfaced to PYTHIA 6, where initial- and final-state radiation parameters are set to a range of values not excluded by the experimental data [72]. The largest relative differences with respect to the reference sample, after full event selections, are used as systematic uncertainties. For high-mass signal samples, this uncertainty is evaluated by varying factorisation/renormalisation scale parameters in the production of signal samples (QCD scale). The uncertainty due to the choice of parton distribution function has a negligible impact for both background and signal, and is not included. An additional uncertainty, arising from the difference in acceptance between 4FS and 5FS H^+ production is evaluated using dedicated signal samples that are generated at leading order with MadGraph [73] interfaced with PYTHIA 8, although the nominal signal samples are generated at NLO. The systematic uncertainties arising from the modelling of the $t\bar{t}$ and signal event generation and the parton shower, as well as from the initial- and final-state radiation, are summarised in table 5.

All of these uncertainties, except for H^+ production, affect only signal and background events where leptons are misidentified as $\tau_{\text{had-vis}}$.

6 Statistical analysis

In order to test the compatibility of the data with background-only and signal+background hypotheses, a profile log-likelihood ratio [74] is used with m_{T} as the discriminating variable. The statistical analysis is based on a binned likelihood function for these distribu-

Source of uncertainty	Normalisation uncertainty
Low-mass H^+	
Generator model ($b\bar{b}W^-H^+$)	9%
Generator model ($b\bar{b}W^+W^-$)	9%
$t\bar{t}$ cross section	6%
Jet production rate (SM and H^+) (QCD scale)	11%
High-mass H^+	
Generator model (H^+)	2–9%
Generator model (SM)	8%
$t\bar{t}$ cross section	6%
Jet production rate (H^+) (QCD scale)	1–2%
Jet production rate (SM) (QCD scale)	11%
H^+ production (4FS vs 5FS)	3–5%

Table 5. Systematic uncertainties arising from $t\bar{t}$ and signal generator modelling, and from the jet production rate. The uncertainties are shown for the $t\bar{t}$ background and the charged Higgs boson signal, for the low-mass and high-mass charged Higgs boson selections separately. The systematic uncertainty of the H^+ yield due to QCD scale and 4FS vs 5FS production was evaluated at masses of 200, 400, and 600 GeV. For all other systematic variations of the H^+ yield, all mass points were considered.

tions. Systematic uncertainties in shape and normalisation, discussed in section 5, are incorporated via nuisance parameters fully correlated amongst the different backgrounds, and the one-sided profile likelihood ratio, $\tilde{q}_\mu$, is used as a test statistic. The parameter of interest, the signal-strength μ, is either $\mathcal{B}(t \to bH^+) \times \mathcal{B}(H^+ \to \tau^+\nu)$ (low-mass search) or $\sigma(pp \to \bar{t}H^+ + X) \times \mathcal{B}(H^+ \to \tau^+\nu)$ (high-mass search). Expected limits are derived using the asymptotic approximation [75].

The nuisance parameters are simultaneously fitted by means of a negative log-likelihood minimisation in both low-mass and high-mass regions in order to ensure that they are well estimated. This is shown in figure 5 for the nuisance parameters that have the largest impact on the fitted μ, denoted $\hat{\mu}$. The black dots indicate how a given nuisance parameter deviates from expectation, while the black error bars indicate how its post-fit uncertainty compares with its nominal uncertainty. In both the low-mass and high-mass searches, the black dots and error bars indicate respectively that none of the nuisance parameters deviate by more than one standard deviation and that their uncertainties are not underestimated. The blue hatched box shows the deviations of the fitted signal-strength parameter after changing a specific nuisance parameter upwards or downwards by its post-fit uncertainty.

The results in figure 5 indicate the relative impact of the systematic uncertainties in the statistical analysis of the low-mass and high-mass searches. For the low-mass search, the most important systematic uncertainties are those related to the measurement of the trigger efficiency and to the simulation of the detector response to $\tau_{\text{had-vis}}$. Since the low-mass search is dominated by the presence of backgrounds with a true τ_{had}, this is consistent

with expectations. For the high-mass search, the most important systematic uncertainties are due to jets misidentified as $\tau_{\text{had-vis}}$, including both the yield and m_{T} distribution of such events, and the next dominant effect is from the true $\tau_{\text{had-vis}}$ background.

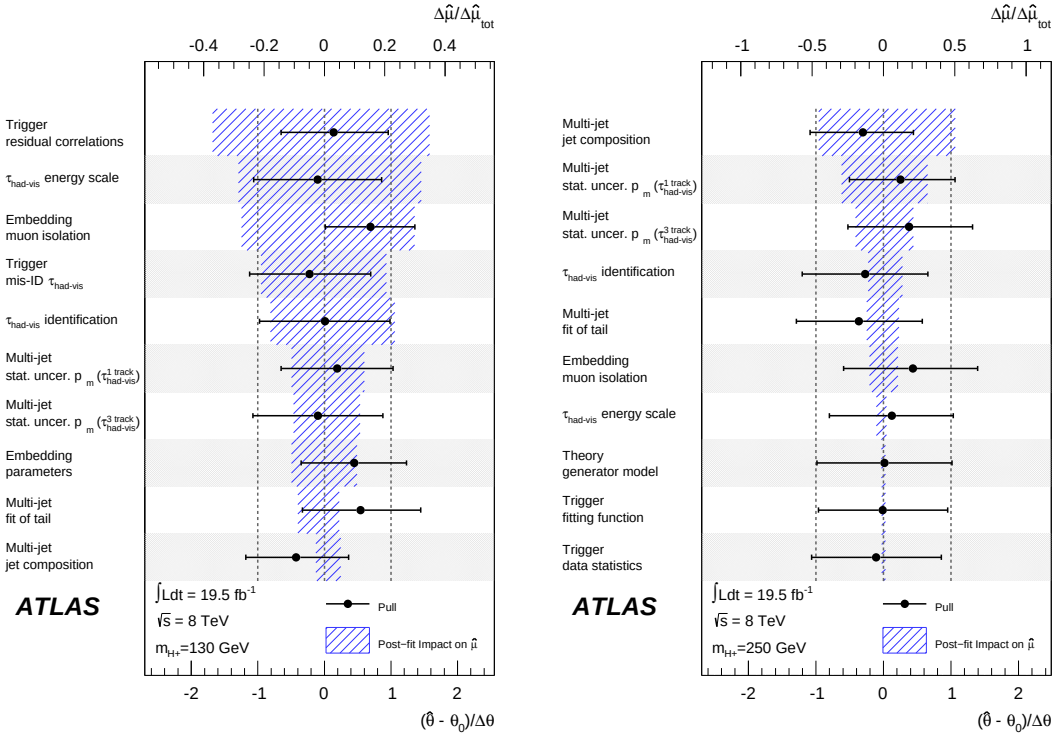

(a) Low-mass H^+ selection

(b) High-mass H^+ selection

Figure 5. Impact of systematic uncertainties on the final observed limits for (a) $m_{H^+} = 130\,\text{GeV}$ and (b) $m_{H^+} = 250\,\text{GeV}$. The systematic uncertainties are ordered (top to bottom) by decreasing impact on the fitted signal strength parameter. The dots, which refer to the bottom horizontal axis, show how each fitted nuisance parameter, $\hat{\theta}$, deviates from its nominal value, θ_0, in terms of standard deviations with respect to its nominal uncertainty, $\Delta\theta$. The solid lines indicate the post-fit uncertainties of each nuisance parameter, also relative to their nominal values. The hatched band, referring to the top horizontal axis, shows the deviations of the fitted signal-strength parameter after changing a specific nuisance parameter upwards or downwards by its post-fit uncertainty ($\Delta\hat{\mu}$) as a fraction of the total uncertainty of the fitted signal-strength parameter ($\Delta\hat{\mu}_{\text{tot}}$).

7 Results

In figure 6, the m_{T} distribution after the final fit is shown. No significant deviation of the data from the SM prediction is observed. For the low-mass charged Higgs boson search, exclusion limits are set on the branching ratio $\mathcal{B}(t \to bH^+) \times \mathcal{B}(H^+ \to \tau^+\nu)$. For the high-mass H^+ search, exclusion limits are set on $\sigma(pp \to \bar{t}H^+ + X) \times \mathcal{B}(H^+ \to \tau^+\nu)$, and are to be understood as applying to the total production cross section times branching ratio of H^+ and H^- combined. Using the binned log-likelihood described in section 6, all exclusion limits are set by rejecting the signal hypothesis at the 95% confidence level (CL)

using the CL_s procedure [76]. These limits are based on the asymptotic distribution of the test statistic [75]. The exclusion limits are shown in figure 7(a) for the low-mass search and in figure 7(b) for the high-mass search. Expected and observed limits agree well and are within the uncertainties over the whole investigated mass range. The limits are in the range between 1.3% and 0.23% for the low-mass search. For the high-mass search, they range from 0.76 pb to 4.5 fb in the mass range 180 GeV $\leq m_{H^+} \leq$ 1000 GeV.

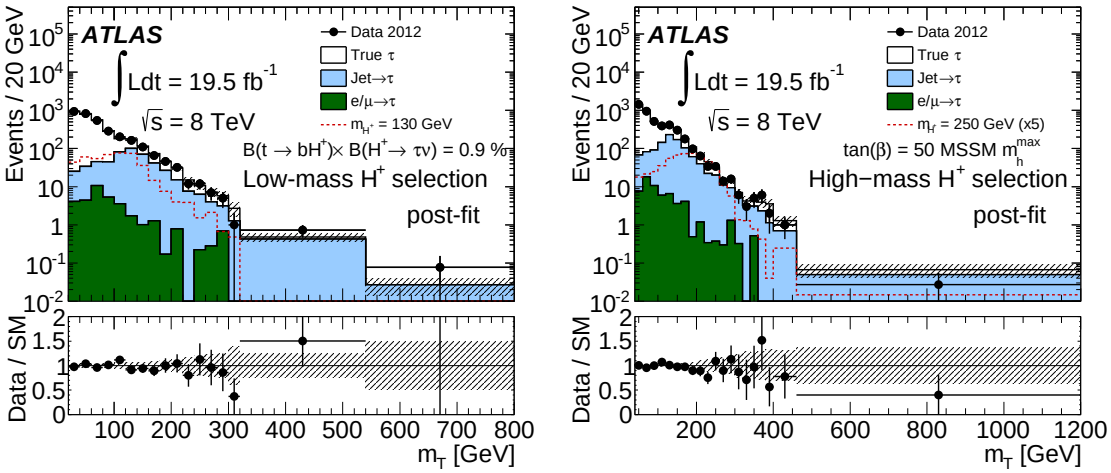

(a) Low-mass H^+ selection

(b) High-mass H^+ selection

Figure 6. Distributions of m_{T} after all selection criteria. The hatched area shows the total post-fit uncertainty for the SM backgrounds. For the (a) low-mass selection, bins are 20 GeV wide up to $m_{\mathrm{T}} = 320$ GeV, then 320–540 GeV and > 540 GeV. For the (b) high-mass selection, bins are 20 GeV wide up to $m_{\mathrm{T}} = 400$ GeV, then 400–460 GeV and > 460 GeV. All bins are normalised to a 20 GeV bin width. For the low-mass search (a), a possible signal contribution with $m_{H^+} = 130$ GeV, and $\mathcal{B}(t \to bH^+) \times \mathcal{B}(H^+ \to \tau^+\nu) = 0.9\%$ is overlaid on top of the SM contributions. For the high-mass search (b), a possible signal contribution with $m_{H^+} = 250$ GeV and $\tan\beta = 50$ in the m_h^{max} scenario of the MSSM, where the corresponding cross section [77] is scaled up by a factor of five, is overlaid on the SM contributions.

The limits on $\mathcal{B}(t \to bH^+) \times \mathcal{B}(H^+ \to \tau^+\nu)$ for the low-mass search and on $\sigma(pp \to \bar{t}H^+ + X) \times \mathcal{B}(H^+ \to \tau^+\nu)$ for the high-mass search are also interpreted in the context of different scenarios of the MSSM [42]. In the m_h^{max} scenario, the mass of the light CP-even Higgs boson h (m_h) is maximised. Interpreting the Higgs boson discovered at the LHC as the h, only a small region of the $m_{H^+} - \tan\beta$ parameter space in this scenario is compatible with the observation. The $m_h^{\mathrm{mod}+}$ and $m_h^{\mathrm{mod}-}$scenarios are modifications of the m_h^{max} scenario. The discovered Higgs boson is interpreted as the h as well but the requirement that m_h be maximal is dropped. This is done by reducing the amount of mixing in the top squark sector compared to the m_h^{max} scenario, leading to a larger region in the parameter space being compatible with the observation. The $m_h^{\mathrm{mod}+}$ and $m_h^{\mathrm{mod}-}$ scenarios only differ in the sign of a parameter.

Interpretations of the 95% CL limits in the m_h^{max}, $m_h^{\mathrm{mod}+}$ and $m_h^{\mathrm{mod}-}$ scenarios are

shown in figure 8. In the low-mass range, almost all values for $\tan\beta > 1$ are excluded in the different scenarios, except for a small region $140\,\text{GeV} \leq m_{H^+} \leq 160\,\text{GeV}$. Values of $\tan\beta$ larger than $45-50$ are excluded in a mass range of $200\,\text{GeV} \leq m_{H^+} \leq 250\,\text{GeV}$. The exclusions in several additional scenarios, not shown here, were also considered. In the light top squark, light stau and tauphobic scenarios, no significant exclusion is achieved in the high-mass search. In the low-mass search, the excluded regions in these scenarios are similar to those shown in figure 8. The limits for the low-mass H^+ search are also interpreted in the low-M_H scenario, where $m_{H^+} \approx 130$ GeV. Instead of excluding areas in the m_{H^+}–$\tan\beta$ plane, limits are interpreted in the $\tan\beta$–μ plane, for $300\,\text{GeV} < \mu < 3500\,\text{GeV}$ and $1.5 < \tan\beta < 9.5$, where μ is the higgsino mass parameter. This model is excluded everywhere where it is tested and where it is well-defined. For the interpretation of the low-mass search, the following relative theoretical uncertainties on $\mathcal{B}(t \to bH^+) \times \mathcal{B}(H^+ \to \tau^+\nu)$ are considered [78–80]: 5% for one-loop electroweak corrections missing from the calculations, 2% for missing two-loop QCD corrections and about 1% (depending on $\tan\beta$) for Δ_b-induced uncertainties, where Δ_b is a correction factor to the running b-quark mass [81]. These uncertainties are added linearly, as recommended by the LHC Higgs cross section working group [79]. For the interpretation of the high-mass search, separate uncertainties are included for the 4FS and 5FS calculations [82]. For the 5FS calculation, the following theoretical uncertainties are taken into account: scale uncertainties of approximately 10–20% that vary with m_{H^+}, the combined uncertainty on the parton distribution function, mass of the b-quark, and strong coupling of approximately 10–15%. For the 4FS calculation, only a scale uncertainty of approximately 30% is taken into account. Owing to the complication arising from the overlap and interference with off-shell $t\bar{t}$ production in the mass range of $m_{H^+} = 180$–$200\,\text{GeV}$, the MSSM interpretation is shown only for $m_{H^+} \geq 200\,\text{GeV}$.

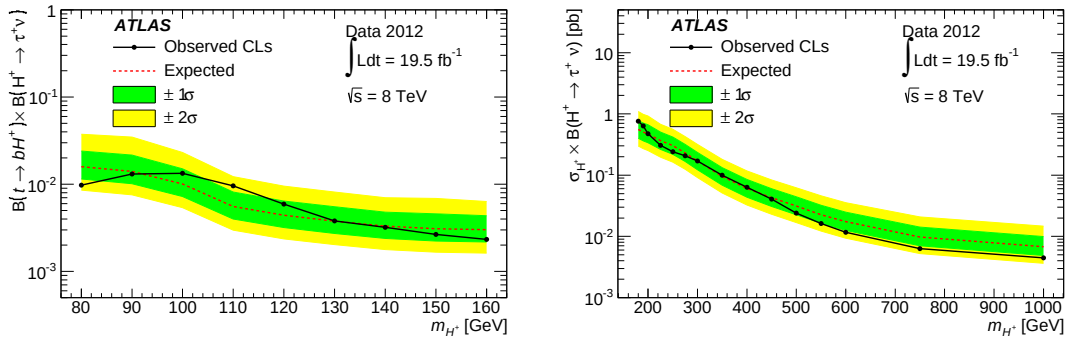

(a) Low-mass H^+ selection

(b) High-mass H^+ selection

Figure 7. Observed and expected 95% CL exclusion limits on the production and decay of (a) low-mass and (b) high-mass charged Higgs bosons. For the low-mass search, the limit is computed for $\mathcal{B}(t \to bH^+) \times \mathcal{B}(H^+ \to \tau^+\nu)$ for charged Higgs boson production from top-quark decays as a function of m_{H^+}. For the high-mass search, the limit is computed for $\sigma(pp \to \bar{t}H^+ + X) \times \mathcal{B}(H^+ \to \tau^+\nu)$, and is to be understood as applying to the total production cross section times branching ratio of H^+ and H^- combined.

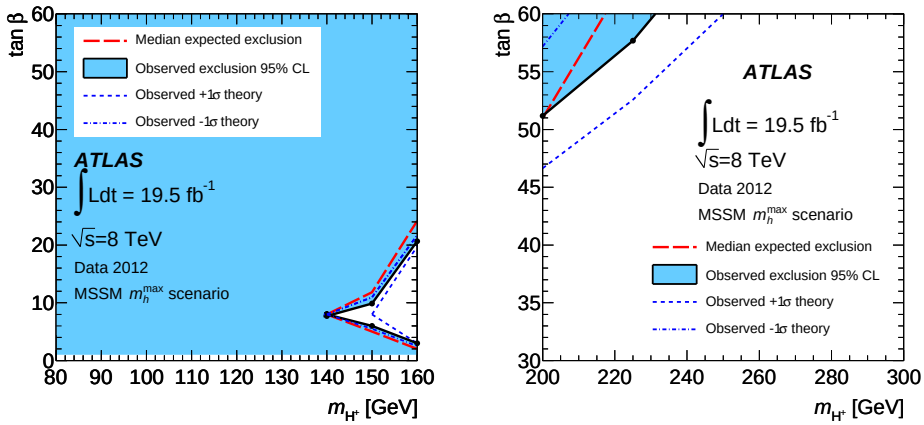

(a) $m_h^{\max}$ scenario, low-mass H^+ selection (b) $m_h^{\max}$ scenario, high-mass H^+ selection

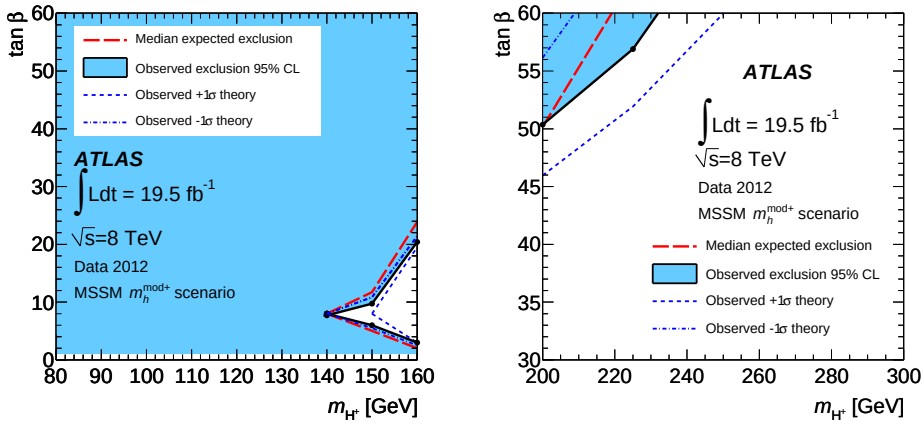

(c) $m_h^{\mathrm{mod}+}$ scenario, low-mass H^+ selection (d) $m_h^{\mathrm{mod}+}$ scenario, high-mass H^+ selection

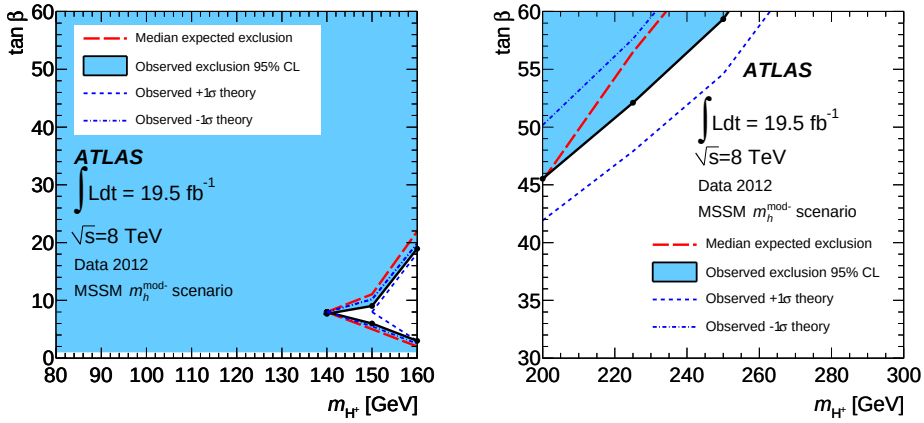

(e) $m_h^{\mathrm{mod}-}$ scenario, low-mass H^+ selection (f) $m_h^{\mathrm{mod}-}$ scenario, high-mass H^+ selection

Figure 8. The 95% CL exclusion limits on $\tan\beta$ as a function of m_{H^+}. Results are shown in the context of different benchmark scenarios of the MSSM for the regions in which reliable theoretical predictions exist. Results are shown for (low-mass, high-mass) H^+ search in the (a, b) $m_h^{\max}$, (c, d) $m_h^{\mathrm{mod}+}$ and (e, f) $m_h^{\mathrm{mod}-}$ scenarios in the left (right) column.

8 Conclusions

Charged Higgs bosons decaying via $H^+ \to \tau^+\nu$ are searched for in $t\bar{t}$ events, in the decay mode $t \to bH^+$ (low-mass search), and for H^+ production in association with a top quark, $pp \to tH^+ + X$ (high-mass search). The analysis makes use of a total of 19.5 fb^{-1} of pp collision data at $\sqrt{s} = 8$ TeV, recorded in 2012 with the ATLAS detector at the LHC. The final state considered in this search is characterised by the presence of a hadronic τ decay, missing transverse momentum, b-tagged jets, a hadronically decaying W boson, as well as the absence of any electrons or muons. Data-driven methods are employed to estimate the dominant background contributions. The data are found to be in agreement with the SM predictions. Upper limits at the 95% confidence level are set on the branching ratio $\mathcal{B}(t \to bH^+) \times \mathcal{B}(H^+ \to \tau^+\nu)$ between 0.23% and 1.3% for a mass range of $m_{H^+} =$ 80–160 GeV, a major improvement over the previous published limits of 0.8–3.4% for the mass range of $m_{H^+} = 90$–160 GeV [18, 19]. For the mass range of $m_{H^+} = 180$–1000 GeV, the first upper limits from ATLAS are set for the production cross section times branching ratio, $\sigma(pp \to \bar{t}H^+ + X) \times \mathcal{B}(H^+ \to \tau^+\nu)$, between 0.76 pb and 4.5 fb. Interpreted in the context of the m_h^{max}, $m_h^{\text{mod+}}$ and $m_h^{\text{mod}-}$ scenarios of the MSSM, the entire parameter space with $\tan\beta > 1$ is excluded for the low-mass range 90 GeV $\leq m_{H^+} \leq$ 140 GeV, and almost all of the parameter space with $\tan\beta > 1$ is excluded for 140 GeV $\leq m_{H^+} \leq$ 160 GeV. For the high-mass range 200 GeV $\leq m_{H^+} \leq$ 250 GeV, a region of parameter space with high $\tan\beta$ is excluded.

9 Acknowledgements

We thank CERN for the very successful operation of the LHC, as well as the support staff from our institutions without whom ATLAS could not be operated efficiently.

We acknowledge the support of ANPCyT, Argentina; YerPhI, Armenia; ARC, Australia; BMWFW and FWF, Austria; ANAS, Azerbaijan; SSTC, Belarus; CNPq and FAPESP, Brazil; NSERC, NRC and CFI, Canada; CERN; CONICYT, Chile; CAS, MOST and NSFC, China; COLCIENCIAS, Colombia; MSMT CR, MPO CR and VSC CR, Czech Republic; DNRF, DNSRC and Lundbeck Foundation, Denmark; EPLANET, ERC and NSRF, European Union; IN2P3-CNRS, CEA-DSM/IRFU, France; GNSF, Georgia; BMBF, DFG, HGF, MPG and AvH Foundation, Germany; GSRT and NSRF, Greece; ISF, MINERVA, GIF, I-CORE and Benoziyo Center, Israel; INFN, Italy; MEXT and JSPS, Japan; CNRST, Morocco; FOM and NWO, Netherlands; BRF and RCN, Norway; MNiSW and NCN, Poland; GRICES and FCT, Portugal; MNE/IFA, Romania; MES of Russia and ROSATOM, Russian Federation; JINR; MSTD, Serbia; MSSR, Slovakia; ARRS and MIZŠ, Slovenia; DST/NRF, South Africa; MINECO, Spain; SRC and Wallenberg Foundation, Sweden; SER, SNSF and Cantons of Bern and Geneva, Switzerland; NSC, Taiwan; TAEK, Turkey; STFC, the Royal Society and Leverhulme Trust, United Kingdom; DOE and NSF, United States of America.

The crucial computing support from all WLCG partners is acknowledged gratefully, in particular from CERN and the ATLAS Tier-1 facilities at TRIUMF (Canada), NDGF

(Denmark, Norway, Sweden), CC-IN2P3 (France), KIT/GridKA (Germany), INFN-CNAF (Italy), NL-T1 (Netherlands), PIC (Spain), ASGC (Taiwan), RAL (UK) and BNL (USA) and in the Tier-2 facilities worldwide.

References

[1] T.D. Lee, *A Theory of Spontaneous T Violation*, *Phys. Rev.* **D 8** (1973) 1226.

[2] T. P. Cheng and L. F. Li, *Neutrino masses, mixings, and oscillations in SU(2)× U(1) models of electroweak interactions*, *Phys. Rev.* **D 22** (1980) 2860.

[3] J. Schechter and J. W. F. Valle, *Neutrino masses in SU(2)× U(1) theories*, *Phys. Rev.* **D 22** (1980) 2227.

[4] G. Lazarides, Q. Shafi and C. Wetterich, *Proton lifetime and fermion masses in an SO(10) model*, *Nucl. Phys.* **B 181** (1981) 287.

[5] R. N. Mohapatra and G. Senjanovic, *Neutrino masses and mixings in gauge models with spontaneous parity violation*, *Phys. Rev.* **D 23** (1981) 165.

[6] M. Magg and C. Wetterich, *Neutrino mass problem and gauge hierarchy*, *Phys. Lett.* **B 94** (1980) 61.

[7] P. Fayet, *Supersymmetry and Weak, Electromagnetic and Strong Interactions*, *Phys. Lett.* **B 64** (1976) 159.

[8] P. Fayet, *Spontaneously Broken Supersymmetric Theories of Weak, Electromagnetic and Strong Interactions*, *Phys. Lett.* **B 69** (1977) 489.

[9] G. R. Farrar and P. Fayet, *Phenomenology of the Production, Decay, and Detection of New Hadronic States Associated with Supersymmetry*, *Phys. Lett.* **B 76** (1978) 575.

[10] P. Fayet, *Relations Between the Masses of the Superpartners of Leptons and Quarks, the Goldstino Couplings and the Neutral Currents*, *Phys. Lett.* **B 84** (1979) 416.

[11] S. Dimopoulos and H. Georgi, *Softly Broken Supersymmetry and SU(5)*, *Nucl. Phys.* **B 193** (1981) 150.

[12] R. Harlander, M. Kramer, and M. Schumacher, *Bottom-quark associated Higgs-boson production: reconciling the four- and five-flavour scheme approach*, [arXiv:1112.3478], (2011).

[13] ATLAS Collaboration, *Measurement of differential production cross-sections for a Z boson in association with b-jets in 7 TeV proton–proton collisions with the ATLAS detector*, *JHEP* **10** (2014) 141, [arXiv:1407.3643].

[14] LHC Higgs Cross Section Working Group, *Handbook of LHC Higgs Cross Sections: 1. Inclusive Observables*, *CERN-2011-002* (2011) [arXiv:1101.0593].

[15] LEP Higgs Working Group for Higgs boson searches, ALEPH Collaboration, DELPHI Collaboration, L3 Collaboration, and OPAL Collaboration, *Search for charged Higgs bosons: Preliminary combined results using LEP data collected at energies up to 209GeV*, [Xiv:hep-ex/0107031], (2001).

[16] CDF Collaboration, T. Aaltonen et al., *Search for charged Higgs bosons in decays of top quarks in p-pbar collisions at* $\sqrt{s} = 1.96$ *TeV*, *Phys. Rev. Lett.* **103** (2009) 101803, [arXiv:0907.1269].

[17] D0 Collaboration, V. Abazov et al., *Search for charged Higgs bosons in top quark decays*, *Phys. Lett.* **B 682** (2009) 278, [arXiv:0908.1811].

[18] ATLAS Collaboration, *Search for charged Higgs bosons through the violation of lepton universality in $t\bar{t}$ events using pp collision data at $\sqrt{s} = 7$ TeV with the ATLAS experiment*, *JHEP* **03** (2013) 076, [arXiv:1212.3572].

[19] CMS Collaboration, *Search for a light charged Higgs boson in top quark decays in pp collisions at $\sqrt{s} = 7$ TeV*, *JHEP* **07** (2012) 143, [arXiv:1205.5736].

[20] E. L. Berger, T. Han, J. Jiang, and T. Plehn, *Associated production of a top quark and a charged Higgs boson*, *Phys.Rev.* **D 71** (2005) 115012, [Xiv:hep-ph/0312286].

[21] ATLAS Collaboration, *The ATLAS Experiment at the CERN Large Hadron Collider*, *JINST* **3** (2008) S08003.

[22] ATLAS Collaboration, *Improved luminosity determination in pp collisions at $\sqrt{s} = 7$ TeV using the ATLAS detector at the LHC*, *Eur. Phys. J.* **C 73** (2013) 2518, [arXiv:1302.4393].

[23] S. Frixione and B. R. Webber, *Matching NLO QCD Computations and Parton Shower Simulations*, *JHEP* **06** (2002) 029, [Xiv:hep-ph/0204244].

[24] S. Frixione, E. Laenen, P. Motylinski, and B. R. Webber, *Single-top production in MC@NLO*, *JHEP* **03** (2006) 092, [Xiv:hep-ph/0512250].

[25] B. P. Kersevan and E. Richter-Was, *The Monte Carlo event generator AcerMC versions 2.0 to 3.8 with interfaces to PYTHIA 6.4, HERWIG 6.5 and ARIADNE 4.1*, *Comput. Phys. Commun.* **184** (2013) 919, [Xiv:hep-ph/0405247].

[26] H.-L. Lai et al., *New parton distributions for collider physics*, *Phys. Rev.* **D 82** (2010) 074024, [arXiv:1007.2241].

[27] G. Corcella et al., *HERWIG 6: An Event generator for hadron emission reactions with interfering gluons (including supersymmetric processes)*, *JHEP* **01** (2001) 010, [Xiv:hep-ph/0011363].

[28] J. Butterworth, J. R. Forshaw, and M. Seymour, *Multiparton interactions in photoproduction at HERA*, *Z. Phys.* **C 72** (1996) 637, [Xiv:hep-ph/9601371].

[29] T. Sjöstrand, S. Mrenna, and P. Z. Skands, *PYTHIA 6.4 Physics and Manual*, *JHEP* **05** (2006) 026, [Xiv:hep-ph/0603175].

[30] M. Aliev et al., *HATHOR – HAdronic Top and Heavy quarks crOss section calculatoR*, *Comput. Phys. Commun.* **182** (2011) 1034, [arXiv:1007.1327].

[31] N. Kidonakis, *Next-to-next-to-leading-order collinear and soft gluon corrections for t-channel single top quark production*, *Phys. Rev.* **D 83** (2011) 091503, [arXiv:1103.2792].

[32] N. Kidonakis, *NNLL resummation for s-channel single top quark production*, *Phys. Rev.* **D 81** (2010) 054028, [arXiv:1001.5034].

[33] N. Kidonakis, *Two-loop soft anomalous dimensions for single top quark associated production with a W^- or H^-*, *Phys. Rev.* **D 82** (2010) 054018, [arXiv:1005.4451].

[34] M. L. Mangano et al., *ALPGEN, a generator for hard multiparton processes in hadronic collisions*, *JHEP* **07** (2003) 001, [Xiv:hep-ph/0206293].

[35] P. M. Nadolsky et al., *Implications of CTEQ global analysis for collider observables*, *Phys. Rev.* **D 78** (2008) 013004, [arXiv:0802.0007].

[36] R. Gavin, Y. Li, F. Petriello, and S. Quackenbush, *W Physics at the LHC with FEWZ 2.1*, *Comput. Phys. Commun.* **184** (2013) 208, [arXiv:1201.5896].

[37] R. Gavin, Y. Li, F. Petriello, and S. Quackenbush, *FEWZ 2.0: A code for hadronic Z production at next-to-next-to-leading order*, *Comput. Phys. Commun.* **182** (2011) 2388, [arXiv:1011.3540].

[38] J. M. Campbell, R. Ellis, and C. Williams, *Vector boson pair production at the LHC*, *JHEP* **07** (2011) 018, [arXiv:1105.0020].

[39] S. Frixione, P. Nason, and C. Oleari, *Matching NLO QCD computations with Parton Shower simulations: the POWHEG method*, *JHEP* **11** (2007) 070, [arXiv:0709.2092].

[40] T. Sjöstrand, S. Mrenna, and P. Z. Skands, *A Brief Introduction to PYTHIA 8.1*, *Comput. Phys. Commun.* **178** (2008) 852, [arXiv:0710.3820].

[41] M. S. Carena, S. Heinemeyer, C. Wagner, and G. Weiglein, *Suggestions for improved benchmark scenarios for Higgs boson searches at LEP-2*, [Xiv:hep-ph/9912223], (1999).

[42] M. Carena et al., *MSSM Higgs Boson Searches at the LHC: Benchmark Scenarios after the Discovery of a Higgs-like Particle*, *Eur. Phys. J.* **C 73** (2013) 2552, [arXiv:1302.7033].

[43] ATLAS Collaboration, *ATLAS tunes of PYTHIA 6 and Pythia 8 for MC11*, *ATL-PHYS-PUB-2011-009* (2011) https://cds.cern.ch/record/1363300.

[44] P. Z. Skands, *Tuning Monte Carlo Generators: The Perugia Tunes*, *Phys. Rev.* **D 82** (2010) 074018, [arXiv:1005.3457].

[45] ATLAS Collaboration, *New ATLAS event generator tunes to 2010 data*, *ATL-PHYS-PUB-2011-008* (2011) https://cdsweb.cern.ch/record/1345343.

[46] Z. Was and P. Golonka, *TAUOLA as tau Monte Carlo for future applications*, *Nucl. Phys. Proc. Suppl.* **144** (2005) 88, [Xiv:hep-ph/0411377].

[47] E. Barberio, B. van Eijk, and Z. Was, *PHOTOS: A universal Monte Carlo for QED radiative corrections in decays*, *Comput. Phys. Commun.* **66** (1991) 115.

[48] GEANT4 Collaboration, S. Agostinelli et al., *GEANT4: A simulation toolkit*, *Nucl. Instrum. Meth.* **A 506** (2003) 250.

[49] ATLAS Collaboration, *The ATLAS Simulation Infrastructure*, *Eur. Phys. J.* **C 70** (2010) 823, [arXiv:1005.4568].

[50] M. Cacciari, G. P. Salam, and G. Soyez, *The anti–k_t jet clustering algorithm*, *JHEP* **04** (2008) 063, [arXiv:0802.1189].

[51] M. Cacciari and G. P. Salam, *Dispelling the N^3 myth for the k_t jet-finder*, *Phys. Lett.* **B 641** (2006) 57, [Xiv:hep-ph/0512210].

[52] D0 Collaboration, V. Abazov et al., *Measurement of the $p\bar{p} \to t\bar{t}$ production cross section at $\sqrt{s} = 1.96$ TeV in the fully hadronic decay channel.*, *Phys. Rev.* **D 76** (2007) 072007, [Xiv:hep-ex/0612040].

[53] ATLAS Collaboration, *Measurement of the b-tag Efficiency in a Sample of Jets Containing Muons with 5 fb^{-1} of Data from the ATLAS Detector*, *ATLAS-CONF-2012-043* (2012) https://cds.cern.ch/record/1435197.

[54] ATLAS Collaboration, *Identification and energy calibration of hadronically decaying tau leptons with the ATLAS experiment in pp collisions at $\sqrt{s}$=8 TeV*, *submitted to Eur. Phys.*

J. C (2014) [arXiv:1412.7086].

[55] L. Breiman, J. Friedman, C. J. Stone, and R. A. Olshen, *Classification and regression trees*. Chapman & Hall, New York, 1984.

[56] Y. Freund and R. E. Schapire, *A decision-theoretic generalization of on-line learning and an application to boosting*, *Journal of Computer and System Sciences* **55** (1997), no. 1 119.

[57] ATLAS Collaboration, *Performance of Missing Transverse Momentum Reconstruction in ATLAS studied in Proton–Proton Collisions recorded in 2012 at 8 TeV*, *ATLAS-CONF-2013-082* (2013) https://cds.cern.ch/record/1570993.

[58] ATLAS Collaboration, *Electron efficiency measurements with the ATLAS detector using the 2012 LHC proton-proton collision data*, *ATLAS-CONF-2014-032* (2014) https://cds.cern.ch/record/1706245.

[59] ATLAS Collaboration, *Electron reconstruction and identification efficiency measurements with the ATLAS detector using the 2011 LHC proton-proton collision data*, *Eur. Phys. J.* **C 74** (2014) 2941, [arXiv:1404.2240].

[60] ATLAS Collaboration, *Measurement of the muon reconstruction performance of the ATLAS detector using 2011 and 2012 LHC proton-proton collision data*, *Eur.Phys.J.* **C 74** (2014) 3130, [arXiv:1407.3935].

[61] ATLAS Collaboration, *Observation and measurement of Higgs boson decays to WW^* with the ATLAS detector*, [arXiv:1412.2641], (2014).

[62] ATLAS Collaboration, *Data-Quality Requirements and Event Cleaning for Jets and Missing Transverse Energy Reconstruction with the ATLAS Detector in Proton–Proton Collisions at a Center-of-Mass Energy of $\sqrt{s} = 7$ TeV*, *ATLAS-CONF-2010-038* (2010) https://cds.cern.ch/record/1277678.

[63] ATLAS Collaboration, *Search for neutral MSSM Higgs bosons decaying to $\tau^+\tau^-$ pairs in proton–proton collisions at $\sqrt{s} = 7$ TeV with the ATLAS detector*, *Phys. Lett.* **B 705** (2011) 174, [arXiv:1107.5003].

[64] ATLAS Collaboration, *Search for charged Higgs bosons decaying via $H^\pm \to \tau\nu$ in top quark pair events using pp collision data at $\sqrt{s} = 7$ TeV with the ATLAS detector*, *JHEP* **06** (2012) 039, [arXiv:1204.2760].

[65] ATLAS Collaboration, *Search for the Standard Model Higgs boson in the H to $\tau^+\tau^-$ decay mode in $\sqrt{s} = 7$ TeV pp collisions with ATLAS*, *JHEP* **09** (2012) 070, [arXiv:1206.5971].

[66] ATLAS Collaboration, *Evidence for the Higgs-boson Yukawa coupling to tau leptons with the ATLAS detector*, [arXiv:1501.0494], (2015).

[67] ATLAS Collaboration, *Determination of the tau energy scale and the associated systematic uncertainty in proton–proton collisions at $\sqrt{s} = 8$ TeV with the ATLAS detector at the LHC in 2012*, *ATLAS-CONF-2013-044* (2013) https://cds.cern.ch/record/1544036.

[68] ATLAS Collaboration, *Jet energy measurement and its systematic uncertainty in proton–proton collisions at $\sqrt{s} = 7$ TeV with the ATLAS detector*, [arXiv:1406.0076], (2014), Accepted by Eur. Phys. J. C.

[69] ATLAS Collaboration, *Calibration of the performance of b-tagging for c and light-flavour jets in the 2012 ATLAS data*, *ATLAS-CONF-2014-046* (2014) https://cds.cern.ch/record/1741020.

[70] ATLAS Collaboration, *Performance of Missing Transverse Momentum Reconstruction in Proton–Proton Collisions at $\sqrt{s} = 7$ TeV with ATLAS*, *Eur. Phys. J.* **C 72** (2012) 1844, [arXiv:1108.5602].

[71] M. Bahr et al, *Herwig++ physics and manual*, *Eur. Phys. J.* **C 58** (2008) 639, [arXiv:0803.0883].

[72] ATLAS Collaboration, *Comparison of Monte Carlo generator predictions for gap fraction and jet multiplicity observables in top-antitop events*, *ATL-PHYS-PUB-2014-005* (2014) https://cds.cern.ch/record/1703034.

[73] J. Alwall et al., *MadGraph 5 : Going Beyond*, *JHEP* **1106** (2011) 128, [arXiv:1106.0522].

[74] ATLAS Collaboration, *Combined search for the Standard Model Higgs boson in pp collisions at $\sqrt{s}$=7 TeV with the ATLAS detector*, *Phys. Rev.* **D 86** (2012) 032003, [arXiv:1207.0319].

[75] G. Cowan, K. Cranmer, E. Gross, and O. Vitells, *Asymptotic formulae for likelihood-based tests of new physics*, *Eur. Phys. J.* **C 71** (2011) 1554, [arXiv:1007.1727].

[76] A. L. Read, *Presentation of search results: The CL(s) technique*, *J. Phys.* **G 28** (2002) 2693.

[77] M. Flechl et al., *Improved cross-section predictions for heavy charged Higgs boson production at the LHC*, [arXiv:1409.5615], (2014).

[78] S. Heinemeyer, W. Hollik, and G. Weiglein, *FeynHiggs: A program for the calculation of the masses of the neutral CP-even Higgs bosons in the MSSM*, *Comput. Phys. Commun.* **124** (2000) 76, [Xiv:hep-ph/9812320].

[79] LHC Higgs Cross Section Working Group, *Handbook of LHC Higgs Cross Sections: 2. Differential Distributions*, *CERN-2012-002* (2012) [arXiv:1201.3084].

[80] S. Dittmaier, M. Kramer, M. Spira, and M. Walser, *Charged-Higgs-boson production at the LHC: NLO supersymmetric QCD corrections*, *Phys.Rev.* **D 83** (2011) 055005, [arXiv:0906.2648].

[81] M. Carena, D. Garcia, U. Nierste, and C. E. M. Wagner, *Effective lagrangian for the $\bar{t}bH^+$ interaction in the MSSM and charged Higgs phenomenology*, *Nucl. Phys.* **B 577** (2000) 88, [Xiv:hep-ph/9912516].

[82] LHC Higgs Cross Section Working Group, *Handbook of LHC Higgs Cross Sections: 3. Higgs Properties*, *CERN-2013-004* (2013) [arXiv:1307.1347].

The ATLAS Collaboration

G. Aad[85], B. Abbott[113], J. Abdallah[152], S. Abdel Khalek[117], O. Abdinov[11], R. Aben[107], B. Abi[114], M. Abolins[90], O.S. AbouZeid[159], H. Abramowicz[154], H. Abreu[153], R. Abreu[30], Y. Abulaiti[147a,147b], B.S. Acharya[165a,165b,a], L. Adamczyk[38a], D.L. Adams[25], J. Adelman[108], S. Adomeit[100], T. Adye[131], T. Agatonovic-Jovin[13a], J.A. Aguilar-Saavedra[126a,126f], M. Agustoni[17], S.P. Ahlen[22], F. Ahmadov[65,b], G. Aielli[134a,134b], H. Akerstedt[147a,147b], T.P.A. Åkesson[81], G. Akimoto[156], A.V. Akimov[96], G.L. Alberghi[20a,20b], J. Albert[170], S. Albrand[55], M.J. Alconada Verzini[71], M. Aleksa[30], I.N. Aleksandrov[65], C. Alexa[26a], G. Alexander[154], G. Alexandre[49], T. Alexopoulos[10], M. Alhroob[113], G. Alimonti[91a], L. Alio[85], J. Alison[31], B.M.M. Allbrooke[18], L.J. Allison[72], P.P. Allport[74], A. Aloisio[104a,104b], A. Alonso[36], F. Alonso[71], C. Alpigiani[76], A. Altheimer[35], B. Alvarez Gonzalez[90], M.G. Alviggi[104a,104b], K. Amako[66], Y. Amaral Coutinho[24a], C. Amelung[23], D. Amidei[89], S.P. Amor Dos Santos[126a,126c], A. Amorim[126a,126b], S. Amoroso[48], N. Amram[154], G. Amundsen[23], C. Anastopoulos[140], L.S. Ancu[49], N. Andari[30], T. Andeen[35], C.F. Anders[58b], G. Anders[30], K.J. Anderson[31], A. Andreazza[91a,91b], V. Andrei[58a], X.S. Anduaga[71], S. Angelidakis[9], I. Angelozzi[107], P. Anger[44], A. Angerami[35], F. Anghinolfi[30], A.V. Anisenkov[109,c], N. Anjos[12], A. Annovi[47], M. Antonelli[47], A. Antonov[98], J. Antos[145b], F. Anulli[133a], M. Aoki[66], L. Aperio Bella[18], G. Arabidze[90], I. Aracena[144], Y. Arai[66], J.P. Araque[126a], A.T.H. Arce[45], F.A. Arduh[71], J-F. Arguin[95], S. Argyropoulos[42], M. Arik[19a], A.J. Armbruster[30], O. Arnaez[30], V. Arnal[82], H. Arnold[48], M. Arratia[28], O. Arslan[21], A. Artamonov[97], G. Artoni[23], S. Asai[156], N. Asbah[42], A. Ashkenazi[154], B. Åsman[147a,147b], L. Asquith[150], K. Assamagan[25], R. Astalos[145a], M. Atkinson[166], N.B. Atlay[142], B. Auerbach[6], K. Augsten[128], M. Aurousseau[146b], G. Avolio[30], B. Axen[15], G. Azuelos[95,d], Y. Azuma[156], M.A. Baak[30], A.E. Baas[58a], C. Bacci[135a,135b], H. Bachacou[137], K. Bachas[155], M. Backes[30], M. Backhaus[30], E. Badescu[26a], P. Bagiacchi[133a,133b], P. Bagnaia[133a,133b], Y. Bai[33a], T. Bain[35], J.T. Baines[131], O.K. Baker[177], P. Balek[129], F. Balli[137], E. Banas[39], Sw. Banerjee[174], A.A.E. Bannoura[176], H.S. Bansil[18], L. Barak[173], S.P. Baranov[96], E.L. Barberio[88], D. Barberis[50a,50b], M. Barbero[85], T. Barillari[101], M. Barisonzi[176], T. Barklow[144], N. Barlow[28], S.L. Barnes[84], B.M. Barnett[131], R.M. Barnett[15], Z. Barnovska[5], A. Baroncelli[135a], G. Barone[49], A.J. Barr[120], F. Barreiro[82], J. Barreiro Guimarães da Costa[57], R. Bartoldus[144], A.E. Barton[72], P. Bartos[145a], V. Bartsch[150], A. Bassalat[117], A. Basye[166], R.L. Bates[53], S.J. Batista[159], J.R. Batley[28], M. Battaglia[138], M. Battistin[30], F. Bauer[137], H.S. Bawa[144,e], J.B. Beacham[111], M.D. Beattie[72], T. Beau[80], P.H. Beauchemin[162], R. Beccherle[124a,124b], P. Bechtle[21], H.P. Beck[17,f], K. Becker[120], S. Becker[100], M. Beckingham[171], C. Becot[117], A.J. Beddall[19c], A. Beddall[19c], S. Bedikian[177], V.A. Bednyakov[65], C.P. Bee[149], L.J. Beemster[107], T.A. Beermann[176], M. Begel[25], K. Behr[120], C. Belanger-Champagne[87], P.J. Bell[49], W.H. Bell[49], G. Bella[154], L. Bellagamba[20a], A. Bellerive[29], M. Bellomo[86], K. Belotskiy[98], O. Beltramello[30], O. Benary[154], D. Benchekroun[136a], K. Bendtz[147a,147b], N. Benekos[166], Y. Benhammou[154], E. Benhar Noccioli[49], J.A. Benitez Garcia[160b], D.P. Benjamin[45], J.R. Bensinger[23], S. Bentvelsen[107], D. Berge[107],

E. Bergeaas Kuutmann[167], N. Berger[5], F. Berghaus[170], J. Beringer[15], C. Bernard[22], N.R. Bernard[86], C. Bernius[110], F.U. Bernlochner[21], T. Berry[77], P. Berta[129], C. Bertella[83], G. Bertoli[147a,147b], F. Bertolucci[124a,124b], C. Bertsche[113], D. Bertsche[113], M.I. Besana[91a], G.J. Besjes[106], O. Bessidskaia Bylund[147a,147b], M. Bessner[42], N. Besson[137], C. Betancourt[48], S. Bethke[101], A.J. Bevan[76], W. Bhimji[46], R.M. Bianchi[125], L. Bianchini[23], M. Bianco[30], O. Biebel[100], S.P. Bieniek[78], K. Bierwagen[54], M. Biglietti[135a], J. Bilbao De Mendizabal[49], H. Bilokon[47], M. Bindi[54], S. Binet[117], A. Bingul[19c], C. Bini[133a,133b], C.W. Black[151], J.E. Black[144], K.M. Black[22], D. Blackburn[139], R.E. Blair[6], J.-B. Blanchard[137], T. Blazek[145a], I. Bloch[42], C. Blocker[23], W. Blum[83,*], U. Blumenschein[54], G.J. Bobbink[107], V.S. Bobrovnikov[109,c], S.S. Bocchetta[81], A. Bocci[45], C. Bock[100], C.R. Boddy[120], M. Boehler[48], T.T. Boek[176], J.A. Bogaerts[30], A.G. Bogdanchikov[109], A. Bogouch[92,*], C. Bohm[147a], V. Boisvert[77], T. Bold[38a], V. Boldea[26a], A.S. Boldyrev[99], M. Bomben[80], M. Bona[76], M. Boonekamp[137], A. Borisov[130], G. Borissov[72], S. Borroni[42], J. Bortfeldt[100], V. Bortolotto[60a], K. Bos[107], D. Boscherini[20a], M. Bosman[12], H. Boterenbrood[107], J. Boudreau[125], J. Bouffard[2], E.V. Bouhova-Thacker[72], D. Boumediene[34], C. Bourdarios[117], N. Bousson[114], S. Boutouil[136d], A. Boveia[31], J. Boyd[30], I.R. Boyko[65], I. Bozic[13a], J. Bracinik[18], A. Brandt[8], G. Brandt[15], O. Brandt[58a], U. Bratzler[157], B. Brau[86], J.E. Brau[116], H.M. Braun[176,*], S.F. Brazzale[165a,165c], B. Brelier[159], K. Brendlinger[122], A.J. Brennan[88], R. Brenner[167], S. Bressler[173], K. Bristow[146c], T.M. Bristow[46], D. Britton[53], F.M. Brochu[28], I. Brock[21], R. Brock[90], J. Bronner[101], G. Brooijmans[35], T. Brooks[77], W.K. Brooks[32b], J. Brosamer[15], E. Brost[116], J. Brown[55], P.A. Bruckman de Renstrom[39], D. Bruncko[145b], R. Bruneliere[48], S. Brunet[61], A. Bruni[20a], G. Bruni[20a], M. Bruschi[20a], L. Bryngemark[81], T. Buanes[14], Q. Buat[143], F. Bucci[49], P. Buchholz[142], A.G. Buckley[53], S.I. Buda[26a], I.A. Budagov[65], F. Buehrer[48], L. Bugge[119], M.K. Bugge[119], O. Bulekov[98], A.C. Bundock[74], H. Burckhart[30], S. Burdin[74], B. Burghgrave[108], S. Burke[131], I. Burmeister[43], E. Busato[34], D. Büscher[48], V. Büscher[83], P. Bussey[53], C.P. Buszello[167], B. Butler[57], J.M. Butler[22], A.I. Butt[3], C.M. Buttar[53], J.M. Butterworth[78], P. Butti[107], W. Buttinger[28], A. Buzatu[53], M. Byszewski[10], S. Cabrera Urbán[168], D. Caforio[20a,20b], O. Cakir[4a], P. Calafiura[15], A. Calandri[137], G. Calderini[80], P. Calfayan[100], L.P. Caloba[24a], D. Calvet[34], S. Calvet[34], R. Camacho Toro[49], S. Camarda[42], D. Cameron[119], L.M. Caminada[15], R. Caminal Armadans[12], S. Campana[30], M. Campanelli[78], A. Campoverde[149], V. Canale[104a,104b], A. Canepa[160a], M. Cano Bret[76], J. Cantero[82], R. Cantrill[126a], T. Cao[40], M.D.M. Capeans Garrido[30], I. Caprini[26a], M. Caprini[26a], M. Capua[37a,37b], R. Caputo[83], R. Cardarelli[134a], T. Carli[30], G. Carlino[104a], L. Carminati[91a,91b], S. Caron[106], E. Carquin[32a], G.D. Carrillo-Montoya[146c], J.R. Carter[28], J. Carvalho[126a,126c], D. Casadei[78], M.P. Casado[12], M. Casolino[12], E. Castaneda-Miranda[146b], A. Castelli[107], V. Castillo Gimenez[168], N.F. Castro[126a], P. Catastini[57], A. Catinaccio[30], J.R. Catmore[119], A. Cattai[30], G. Cattani[134a,134b], J. Caudron[83], V. Cavaliere[166], D. Cavalli[91a], M. Cavalli-Sforza[12], V. Cavasinni[124a,124b], F. Ceradini[135a,135b], B.C. Cerio[45], K. Cerny[129], A.S. Cerqueira[24b], A. Cerri[150], L. Cerrito[76], F. Cerutti[15], M. Cerv[30], A. Cervelli[17], S.A. Cetin[19b], A. Chafaq[136a], D. Chakraborty[108], I. Chalupkova[129], P. Chang[166], B. Chapleau[87], J.D. Chapman[28],

D. Charfeddine[117], D.G. Charlton[18], C.C. Chau[159], C.A. Chavez Barajas[150], S. Cheatham[153], A. Chegwidden[90], S. Chekanov[6], S.V. Chekulaev[160a], G.A. Chelkov[65,g], M.A. Chelstowska[89], C. Chen[64], H. Chen[25], K. Chen[149], L. Chen[33d,h], S. Chen[33c], X. Chen[33f], Y. Chen[67], H.C. Cheng[89], Y. Cheng[31], A. Cheplakov[65], E. Cheremushkina[130], R. Cherkaoui El Moursli[136e], V. Chernyatin[25,*], E. Cheu[7], L. Chevalier[137], V. Chiarella[47], G. Chiefari[104a,104b], J.T. Childers[6], A. Chilingarov[72], G. Chiodini[73a], A.S. Chisholm[18], R.T. Chislett[78], A. Chitan[26a], M.V. Chizhov[65], S. Chouridou[9], B.K.B. Chow[100], D. Chromek-Burckhart[30], M.L. Chu[152], J. Chudoba[127], J.J. Chwastowski[39], L. Chytka[115], G. Ciapetti[133a,133b], A.K. Ciftci[4a], R. Ciftci[4a], D. Cinca[53], V. Cindro[75], A. Ciocio[15], Z.H. Citron[173], M. Citterio[91a], M. Ciubancan[26a], A. Clark[49], P.J. Clark[46], R.N. Clarke[15], W. Cleland[125], J.C. Clemens[85], C. Clement[147a,147b], Y. Coadou[85], M. Cobal[165a,165c], A. Coccaro[139], J. Cochran[64], L. Coffey[23], J.G. Cogan[144], B. Cole[35], S. Cole[108], A.P. Colijn[107], J. Collot[55], T. Colombo[58c], G. Compostella[101], P. Conde Muiño[126a,126b], E. Coniavitis[48], S.H. Connell[146b], I.A. Connelly[77], S.M. Consonni[91a,91b], V. Consorti[48], S. Constantinescu[26a], C. Conta[121a,121b], G. Conti[30], F. Conventi[104a,i], M. Cooke[15], B.D. Cooper[78], A.M. Cooper-Sarkar[120], N.J. Cooper-Smith[77], K. Copic[15], T. Cornelissen[176], M. Corradi[20a], F. Corriveau[87,j], A. Corso-Radu[164], A. Cortes-Gonzalez[12], G. Cortiana[101], G. Costa[91a], M.J. Costa[168], D. Costanzo[140], D. Côté[8], G. Cottin[28], G. Cowan[77], B.E. Cox[84], K. Cranmer[110], G. Cree[29], S. Crépé-Renaudin[55], F. Crescioli[80], W.A. Cribbs[147a,147b], M. Crispin Ortuzar[120], M. Cristinziani[21], V. Croft[106], G. Crosetti[37a,37b], T. Cuhadar Donszelmann[140], J. Cummings[177], M. Curatolo[47], C. Cuthbert[151], H. Czirr[142], P. Czodrowski[3], S. D'Auria[53], M. D'Onofrio[74], M.J. Da Cunha Sargedas De Sousa[126a,126b], C. Da Via[84], W. Dabrowski[38a], A. Dafinca[120], T. Dai[89], O. Dale[14], F. Dallaire[95], C. Dallapiccola[86], M. Dam[36], A.C. Daniells[18], M. Danninger[169], M. Dano Hoffmann[137], V. Dao[48], G. Darbo[50a], S. Darmora[8], J. Dassoulas[74], A. Dattagupta[61], W. Davey[21], C. David[170], T. Davidek[129], E. Davies[120,k], M. Davies[154], O. Davignon[80], A.R. Davison[78], P. Davison[78], Y. Davygora[58a], E. Dawe[143], I. Dawson[140], R.K. Daya-Ishmukhametova[86], K. De[8], R. de Asmundis[104a], S. De Castro[20a,20b], S. De Cecco[80], N. De Groot[106], P. de Jong[107], H. De la Torre[82], F. De Lorenzi[64], L. De Nooij[107], D. De Pedis[133a], A. De Salvo[133a], U. De Sanctis[150], A. De Santo[150], J.B. De Vivie De Regie[117], W.J. Dearnaley[72], R. Debbe[25], C. Debenedetti[138], B. Dechenaux[55], D.V. Dedovich[65], I. Deigaard[107], J. Del Peso[82], T. Del Prete[124a,124b], F. Deliot[137], C.M. Delitzsch[49], M. Deliyergiyev[75], A. Dell'Acqua[30], L. Dell'Asta[22], M. Dell'Orso[124a,124b], M. Della Pietra[104a,i], D. della Volpe[49], M. Delmastro[5], P.A. Delsart[55], C. Deluca[107], D.A. DeMarco[159], S. Demers[177], M. Demichev[65], A. Demilly[80], S.P. Denisov[130], D. Derendarz[39], J.E. Derkaoui[136d], F. Derue[80], P. Dervan[74], K. Desch[21], C. Deterre[42], P.O. Deviveiros[30], A. Dewhurst[131], S. Dhaliwal[107], A. Di Ciaccio[134a,134b], L. Di Ciaccio[5], A. Di Domenico[133a,133b], C. Di Donato[104a,104b], A. Di Girolamo[30], B. Di Girolamo[30], A. Di Mattia[153], B. Di Micco[135a,135b], R. Di Nardo[47], A. Di Simone[48], R. Di Sipio[20a,20b], D. Di Valentino[29], F.A. Dias[46], M.A. Diaz[32a], E.B. Diehl[89], J. Dietrich[16], T.A. Dietzsch[58a], S. Diglio[85], A. Dimitrievska[13a], J. Dingfelder[21], P. Dita[26a], S. Dita[26a], F. Dittus[30], F. Djama[85], T. Djobava[51b], J.I. Djuvsland[58a], M.A.B. do Vale[24c],

D. Dobos[30], C. Doglioni[49], T. Doherty[53], T. Dohmae[156], J. Dolejsi[129], Z. Dolezal[129], B.A. Dolgoshein[98,*], M. Donadelli[24d], S. Donati[124a,124b], P. Dondero[121a,121b], J. Donini[34], J. Dopke[131], A. Doria[104a], M.T. Dova[71], A.T. Doyle[53], M. Dris[10], J. Dubbert[89], S. Dube[15], E. Dubreuil[34], E. Duchovni[173], G. Duckeck[100], O.A. Ducu[26a], D. Duda[176], A. Dudarev[30], F. Dudziak[64], L. Duflot[117], L. Duguid[77], M. Dührssen[30], M. Dunford[58a], H. Duran Yildiz[4a], M. Düren[52], A. Durglishvili[51b], D. Duschinger[44], M. Dwuznik[38a], M. Dyndal[38a], J. Ebke[100], W. Edson[2], N.C. Edwards[46], W. Ehrenfeld[21], T. Eifert[30], G. Eigen[14], K. Einsweiler[15], T. Ekelof[167], M. El Kacimi[136c], M. Ellert[167], S. Elles[5], F. Ellinghaus[83], A.A. Elliot[170], N. Ellis[30], J. Elmsheuser[100], M. Elsing[30], D. Emeliyanov[131], Y. Enari[156], O.C. Endner[83], M. Endo[118], R. Engelmann[149], J. Erdmann[43], A. Ereditato[17], D. Eriksson[147a], G. Ernis[176], J. Ernst[2], M. Ernst[25], J. Ernwein[137], S. Errede[166], E. Ertel[83], M. Escalier[117], H. Esch[43], C. Escobar[125], B. Esposito[47], A.I. Etienvre[137], E. Etzion[154], H. Evans[61], A. Ezhilov[123], L. Fabbri[20a,20b], G. Facini[31], R.M. Fakhrutdinov[130], S. Falciano[133a], R.J. Falla[78], J. Faltova[129], Y. Fang[33a], M. Fanti[91a,91b], A. Farbin[8], A. Farilla[135a], T. Farooque[12], S. Farrell[15], S.M. Farrington[171], P. Farthouat[30], F. Fassi[136e], P. Fassnacht[30], D. Fassouliotis[9], A. Favareto[50a,50b], L. Fayard[117], P. Federic[145a], O.L. Fedin[123,l], W. Fedorko[169], S. Feigl[30], L. Feligioni[85], C. Feng[33d], E.J. Feng[6], H. Feng[89], A.B. Fenyuk[130], P. Fernandez Martinez[168], S. Fernandez Perez[30], S. Ferrag[53], J. Ferrando[53], A. Ferrari[167], P. Ferrari[107], R. Ferrari[121a], D.E. Ferreira de Lima[53], A. Ferrer[168], D. Ferrere[49], C. Ferretti[89], A. Ferretto Parodi[50a,50b], M. Fiascaris[31], F. Fiedler[83], A. Filipčič[75], M. Filipuzzi[42], F. Filthaut[106], M. Fincke-Keeler[170], K.D. Finelli[151], M.C.N. Fiolhais[126a,126c], L. Fiorini[168], A. Firan[40], A. Fischer[2], J. Fischer[176], W.C. Fisher[90], E.A. Fitzgerald[23], M. Flechl[48], I. Fleck[142], P. Fleischmann[89], S. Fleischmann[176], G.T. Fletcher[140], G. Fletcher[76], T. Flick[176], A. Floderus[81], L.R. Flores Castillo[60a], M.J. Flowerdew[101], A. Formica[137], A. Forti[84], D. Fournier[117], H. Fox[72], S. Fracchia[12], P. Francavilla[80], M. Franchini[20a,20b], S. Franchino[30], D. Francis[30], L. Franconi[119], M. Franklin[57], M. Fraternali[121a,121b], S.T. French[28], C. Friedrich[42], F. Friedrich[44], D. Froidevaux[30], J.A. Frost[120], C. Fukunaga[157], E. Fullana Torregrosa[83], B.G. Fulsom[144], J. Fuster[168], C. Gabaldon[55], O. Gabizon[176], A. Gabrielli[20a,20b], A. Gabrielli[133a,133b], S. Gadatsch[107], S. Gadomski[49], G. Gagliardi[50a,50b], P. Gagnon[61], C. Galea[106], B. Galhardo[126a,126c], E.J. Gallas[120], B.J. Gallop[131], P. Gallus[128], G. Galster[36], K.K. Gan[111], J. Gao[33b], Y.S. Gao[144,e], F.M. Garay Walls[46], F. Garberson[177], C. García[168], J.E. García Navarro[168], M. Garcia-Sciveres[15], R.W. Gardner[31], N. Garelli[144], V. Garonne[30], C. Gatti[47], G. Gaudio[121a], B. Gaur[142], L. Gauthier[95], P. Gauzzi[133a,133b], I.L. Gavrilenko[96], C. Gay[169], G. Gaycken[21], E.N. Gazis[10], P. Ge[33d], Z. Gecse[169], C.N.P. Gee[131], D.A.A. Geerts[107], Ch. Geich-Gimbel[21], K. Gellerstedt[147a,147b], C. Gemme[50a], A. Gemmell[53], M.H. Genest[55], S. Gentile[133a,133b], M. George[54], S. George[77], D. Gerbaudo[164], A. Gershon[154], H. Ghazlane[136b], N. Ghodbane[34], B. Giacobbe[20a], S. Giagu[133a,133b], V. Giangiobbe[12], P. Giannetti[124a,124b], F. Gianotti[30], B. Gibbard[25], S.M. Gibson[77], M. Gilchriese[15], T.P.S. Gillam[28], D. Gillberg[30], G. Gilles[34], D.M. Gingrich[3,d], N. Giokaris[9], M.P. Giordani[165a,165c], R. Giordano[104a,104b], F.M. Giorgi[20a], F.M. Giorgi[16], P.F. Giraud[137], D. Giugni[91a], C. Giuliani[48], M. Giulini[58b],

B.K. Gjelsten[119], S. Gkaitatzis[155], I. Gkialas[155], E.L. Gkougkousis[117], L.K. Gladilin[99], C. Glasman[82], J. Glatzer[30], P.C.F. Glaysher[46], A. Glazov[42], G.L. Glonti[62], M. Goblirsch-Kolb[101], J.R. Goddard[76], J. Godlewski[30], S. Goldfarb[89], T. Golling[49], D. Golubkov[130], A. Gomes[126a,126b,126d], L.S. Gomez Fajardo[42], R. Gonçalo[126a], J. Goncalves Pinto Firmino Da Costa[137], L. Gonella[21], S. González de la Hoz[168], G. Gonzalez Parra[12], S. Gonzalez-Sevilla[49], L. Goossens[30], P.A. Gorbounov[97], H.A. Gordon[25], I. Gorelov[105], B. Gorini[30], E. Gorini[73a,73b], A. Gorišek[75], E. Gornicki[39], A.T. Goshaw[45], C. Gössling[43], M.I. Gostkin[65], M. Gouighri[136a], D. Goujdami[136c], M.P. Goulette[49], A.G. Goussiou[139], C. Goy[5], H.M.X. Grabas[138], L. Graber[54], I. Grabowska-Bold[38a], P. Grafström[20a,20b], K-J. Grahn[42], J. Gramling[49], E. Gramstad[119], S. Grancagnolo[16], V. Grassi[149], V. Gratchev[123], H.M. Gray[30], E. Graziani[135a], O.G. Grebenyuk[123], Z.D. Greenwood[79,m], K. Gregersen[78], I.M. Gregor[42], P. Grenier[144], J. Griffiths[8], A.A. Grillo[138], K. Grimm[72], S. Grinstein[12,n], Ph. Gris[34], Y.V. Grishkevich[99], J.-F. Grivaz[117], J.P. Grohs[44], A. Grohsjean[42], E. Gross[173], J. Grosse-Knetter[54], G.C. Grossi[134a,134b], Z.J. Grout[150], L. Guan[33b], J. Guenther[128], F. Guescini[49], D. Guest[177], O. Gueta[154], C. Guicheney[34], E. Guido[50a,50b], T. Guillemin[117], S. Guindon[2], U. Gul[53], C. Gumpert[44], J. Guo[35], S. Gupta[120], P. Gutierrez[113], N.G. Gutierrez Ortiz[53], C. Gutschow[78], N. Guttman[154], C. Guyot[137], C. Gwenlan[120], C.B. Gwilliam[74], A. Haas[110], C. Haber[15], H.K. Hadavand[8], N. Haddad[136e], P. Haefner[21], S. Hageböck[21], Z. Hajduk[39], H. Hakobyan[178], M. Haleem[42], D. Hall[120], G. Halladjian[90], G.D. Hallewell[85], K. Hamacher[176], P. Hamal[115], K. Hamano[170], M. Hamer[54], A. Hamilton[146a], S. Hamilton[162], G.N. Hamity[146c], P.G. Hamnett[42], L. Han[33b], K. Hanagaki[118], K. Hanawa[156], M. Hance[15], P. Hanke[58a], R. Hanna[137], J.B. Hansen[36], J.D. Hansen[36], P.H. Hansen[36], K. Hara[161], A.S. Hard[174], T. Harenberg[176], F. Hariri[117], S. Harkusha[92], R.D. Harrington[46], O.M. Harris[139], P.F. Harrison[171], F. Hartjes[107], M. Hasegawa[67], S. Hasegawa[103], Y. Hasegawa[141], A. Hasib[113], S. Hassani[137], S. Haug[17], M. Hauschild[30], R. Hauser[90], M. Havranek[127], C.M. Hawkes[18], R.J. Hawkings[30], A.D. Hawkins[81], T. Hayashi[161], D. Hayden[90], C.P. Hays[120], J.M. Hays[76], H.S. Hayward[74], S.J. Haywood[131], S.J. Head[18], T. Heck[83], V. Hedberg[81], L. Heelan[8], S. Heim[122], T. Heim[176], B. Heinemann[15], L. Heinrich[110], J. Hejbal[127], L. Helary[22], C. Heller[100], M. Heller[30], S. Hellman[147a,147b], D. Hellmich[21], C. Helsens[30], J. Henderson[120], R.C.W. Henderson[72], Y. Heng[174], C. Hengler[42], A. Henrichs[177], A.M. Henriques Correia[30], S. Henrot-Versille[117], G.H. Herbert[16], Y. Hernández Jiménez[168], R. Herrberg-Schubert[16], G. Herten[48], R. Hertenberger[100], L. Hervas[30], G.G. Hesketh[78], N.P. Hessey[107], R. Hickling[76], E. Higón-Rodriguez[168], E. Hill[170], J.C. Hill[28], K.H. Hiller[42], S.J. Hillier[18], I. Hinchliffe[15], E. Hines[122], R.R. Hinman[15], M. Hirose[158], D. Hirschbuehl[176], J. Hobbs[149], N. Hod[107], M.C. Hodgkinson[140], P. Hodgson[140], A. Hoecker[30], M.R. Hoeferkamp[105], F. Hoenig[100], D. Hoffmann[85], M. Hohlfeld[83], T.R. Holmes[15], T.M. Hong[122], L. Hooft van Huysduynen[110], W.H. Hopkins[116], Y. Horii[103], A.J. Horton[143], J-Y. Hostachy[55], S. Hou[152], A. Hoummada[136a], J. Howard[120], J. Howarth[42], M. Hrabovsky[115], I. Hristova[16], J. Hrivnac[117], T. Hryn'ova[5], A. Hrynevich[93], C. Hsu[146c], P.J. Hsu[152,o], S.-C. Hsu[139], D. Hu[35], X. Hu[89], Y. Huang[42], Z. Hubacek[30], F. Hubaut[85],

F. Huegging[21], T.B. Huffman[120], E.W. Hughes[35], G. Hughes[72], M. Huhtinen[30], T.A. Hülsing[83], M. Hurwitz[15], N. Huseynov[65,b], J. Huston[90], J. Huth[57], G. Iacobucci[49], G. Iakovidis[10], I. Ibragimov[142], L. Iconomidou-Fayard[117], E. Ideal[177], Z. Idrissi[136e], P. Iengo[104a], O. Igonkina[107], T. Iizawa[172], Y. Ikegami[66], K. Ikematsu[142], M. Ikeno[66], Y. Ilchenko[31,p], D. Iliadis[155], N. Ilic[159], Y. Inamaru[67], T. Ince[101], P. Ioannou[9], M. Iodice[135a], K. Iordanidou[9], V. Ippolito[57], A. Irles Quiles[168], C. Isaksson[167], M. Ishino[68], M. Ishitsuka[158], R. Ishmukhametov[111], C. Issever[120], S. Istin[19a], J.M. Iturbe Ponce[84], R. Iuppa[134a,134b], J. Ivarsson[81], W. Iwanski[39], H. Iwasaki[66], J.M. Izen[41], V. Izzo[104a], B. Jackson[122], M. Jackson[74], P. Jackson[1], M.R. Jaekel[30], V. Jain[2], K. Jakobs[48], S. Jakobsen[30], T. Jakoubek[127], J. Jakubek[128], D.O. Jamin[152], D.K. Jana[79], E. Jansen[78], H. Jansen[30], J. Janssen[21], M. Janus[171], G. Jarlskog[81], N. Javadov[65,b], T. Javůrek[48], L. Jeanty[15], J. Jejelava[51a,q], G.-Y. Jeng[151], D. Jennens[88], P. Jenni[48,r], J. Jentzsch[43], C. Jeske[171], S. Jézéquel[5], H. Ji[174], J. Jia[149], Y. Jiang[33b], M. Jimenez Belenguer[42], S. Jin[33a], A. Jinaru[26a], O. Jinnouchi[158], M.D. Joergensen[36], P. Johansson[140], K.A. Johns[7], K. Jon-And[147a,147b], G. Jones[171], R.W.L. Jones[72], T.J. Jones[74], J. Jongmanns[58a], P.M. Jorge[126a,126b], K.D. Joshi[84], J. Jovicevic[148], X. Ju[174], C.A. Jung[43], P. Jussel[62], A. Juste Rozas[12,n], M. Kaci[168], A. Kaczmarska[39], M. Kado[117], H. Kagan[111], M. Kagan[144], E. Kajomovitz[45], C.W. Kalderon[120], S. Kama[40], A. Kamenshchikov[130], N. Kanaya[156], M. Kaneda[30], S. Kaneti[28], V.A. Kantserov[98], J. Kanzaki[66], B. Kaplan[110], A. Kapliy[31], D. Kar[53], K. Karakostas[10], A. Karamaoun[3], N. Karastathis[10], M.J. Kareem[54], M. Karnevskiy[83], S.N. Karpov[65], Z.M. Karpova[65], K. Karthik[110], V. Kartvelishvili[72], A.N. Karyukhin[130], L. Kashif[174], G. Kasieczka[58b], R.D. Kass[111], A. Kastanas[14], Y. Kataoka[156], A. Katre[49], J. Katzy[42], V. Kaushik[7], K. Kawagoe[70], T. Kawamoto[156], G. Kawamura[54], S. Kazama[156], V.F. Kazanin[109], M.Y. Kazarinov[65], R. Keeler[170], R. Kehoe[40], M. Keil[54], J.S. Keller[42], J.J. Kempster[77], H. Keoshkerian[5], O. Kepka[127], B.P. Kerševan[75], S. Kersten[176], K. Kessoku[156], J. Keung[159], R.A. Keyes[87], F. Khalil-zada[11], H. Khandanyan[147a,147b], A. Khanov[114], A. Kharlamov[109], A. Khodinov[98], A. Khomich[58a], T.J. Khoo[28], G. Khoriauli[21], V. Khovanskiy[97], E. Khramov[65], J. Khubua[51b], H.Y. Kim[8], H. Kim[147a,147b], S.H. Kim[161], N. Kimura[155], O. Kind[16], B.T. King[74], M. King[168], R.S.B. King[120], S.B. King[169], J. Kirk[131], A.E. Kiryunin[101], T. Kishimoto[67], D. Kisielewska[38a], F. Kiss[48], K. Kiuchi[161], E. Kladiva[145b], M. Klein[74], U. Klein[74], K. Kleinknecht[83], P. Klimek[147a,147b], A. Klimentov[25], R. Klingenberg[43], J.A. Klinger[84], T. Klioutchnikova[30], P.F. Klok[106], E.-E. Kluge[58a], P. Kluit[107], S. Kluth[101], E. Kneringer[62], E.B.F.G. Knoops[85], A. Knue[53], D. Kobayashi[158], T. Kobayashi[156], M. Kobel[44], M. Kocian[144], P. Kodys[129], T. Koffas[29], E. Koffeman[107], L.A. Kogan[120], S. Kohlmann[176], Z. Kohout[128], T. Kohriki[66], T. Koi[144], H. Kolanoski[16], I. Koletsou[5], J. Koll[90], A.A. Komar[96,*], Y. Komori[156], T. Kondo[66], N. Kondrashova[42], K. Köneke[48], A.C. König[106], S. König[83], T. Kono[66,s], R. Konoplich[110,t], N. Konstantinidis[78], R. Kopeliansky[153], S. Koperny[38a], L. Köpke[83], A.K. Kopp[48], K. Korcyl[39], K. Kordas[155], A. Korn[78], A.A. Korol[109,c], I. Korolkov[12], E.V. Korolkova[140], V.A. Korotkov[130], O. Kortner[101], S. Kortner[101], V.V. Kostyukhin[21], V.M. Kotov[65], A. Kotwal[45], A. Kourkoumeli-Charalampidi[155], C. Kourkoumelis[9], V. Kouskoura[25], A. Koutsman[160a], R. Kowalewski[170], T.Z. Kowalski[38a], W. Kozanecki[137],

A.S. Kozhin[130], V.A. Kramarenko[99], G. Kramberger[75], D. Krasnopevtsev[98], M.W. Krasny[80], A. Krasznahorkay[30], J.K. Kraus[21], A. Kravchenko[25], S. Kreiss[110], M. Kretz[58c], J. Kretzschmar[74], K. Kreutzfeldt[52], P. Krieger[159], K. Krizka[31], K. Kroeninger[43], H. Kroha[101], J. Kroll[122], J. Kroseberg[21], J. Krstic[13a], U. Kruchonak[65], H. Krüger[21], N. Krumnack[64], Z.V. Krumshteyn[65], A. Kruse[174], M.C. Kruse[45], M. Kruskal[22], T. Kubota[88], H. Kucuk[78], S. Kuday[4c], S. Kuehn[48], A. Kugel[58c], F. Kuger[175], A. Kuhl[138], T. Kuhl[42], V. Kukhtin[65], Y. Kulchitsky[92], S. Kuleshov[32b], M. Kuna[133a,133b], T. Kunigo[68], A. Kupco[127], H. Kurashige[67], Y.A. Kurochkin[92], R. Kurumida[67], V. Kus[127], E.S. Kuwertz[148], M. Kuze[158], J. Kvita[115], D. Kyriazopoulos[140], A. La Rosa[49], L. La Rotonda[37a,37b], C. Lacasta[168], F. Lacava[133a,133b], J. Lacey[29], H. Lacker[16], D. Lacour[80], V.R. Lacuesta[168], E. Ladygin[65], R. Lafaye[5], B. Laforge[80], T. Lagouri[177], S. Lai[48], H. Laier[58a], L. Lambourne[78], S. Lammers[61], C.L. Lampen[7], W. Lampl[7], E. Lançon[137], U. Landgraf[48], M.P.J. Landon[76], V.S. Lang[58a], A.J. Lankford[164], F. Lanni[25], K. Lantzsch[30], S. Laplace[80], C. Lapoire[21], J.F. Laporte[137], T. Lari[91a], F. Lasagni Manghi[20a,20b], M. Lassnig[30], P. Laurelli[47], W. Lavrijsen[15], A.T. Law[138], P. Laycock[74], O. Le Dortz[80], E. Le Guirriec[85], E. Le Menedeu[12], T. LeCompte[6], F. Ledroit-Guillon[55], C.A. Lee[146b], H. Lee[107], S.C. Lee[152], L. Lee[1], G. Lefebvre[80], M. Lefebvre[170], F. Legger[100], C. Leggett[15], A. Lehan[74], G. Lehmann Miotto[30], X. Lei[7], W.A. Leight[29], A. Leisos[155], A.G. Leister[177], M.A.L. Leite[24d], R. Leitner[129], D. Lellouch[173], B. Lemmer[54], K.J.C. Leney[78], T. Lenz[21], G. Lenzen[176], B. Lenzi[30], R. Leone[7], S. Leone[124a,124b], C. Leonidopoulos[46], S. Leontsinis[10], C. Leroy[95], C.G. Lester[28], C.M. Lester[122], M. Levchenko[123], J. Levêque[5], D. Levin[89], L.J. Levinson[173], M. Levy[18], A. Lewis[120], A.M. Leyko[21], M. Leyton[41], B. Li[33b,u], B. Li[85], H. Li[149], H.L. Li[31], L. Li[45], L. Li[33e], S. Li[45], Y. Li[33c,v], Z. Liang[138], H. Liao[34], B. Liberti[134a], P. Lichard[30], K. Lie[166], J. Liebal[21], W. Liebig[14], C. Limbach[21], A. Limosani[151], S.C. Lin[152,w], T.H. Lin[83], F. Linde[107], B.E. Lindquist[149], J.T. Linnemann[90], E. Lipeles[122], A. Lipniacka[14], M. Lisovyi[42], T.M. Liss[166], D. Lissauer[25], A. Lister[169], A.M. Litke[138], B. Liu[152], D. Liu[152], J. Liu[85], J.B. Liu[33b], K. Liu[33b,x], L. Liu[89], M. Liu[45], M. Liu[33b], Y. Liu[33b], M. Livan[121a,121b], A. Lleres[55], J. Llorente Merino[82], S.L. Lloyd[76], F. Lo Sterzo[152], E. Lobodzinska[42], P. Loch[7], W.S. Lockman[138], F.K. Loebinger[84], A.E. Loevschall-Jensen[36], A. Loginov[177], T. Lohse[16], K. Lohwasser[42], M. Lokajicek[127], B.A. Long[22], J.D. Long[89], R.E. Long[72], K.A. Looper[111], L. Lopes[126a], D. Lopez Mateos[57], B. Lopez Paredes[140], I. Lopez Paz[12], J. Lorenz[100], N. Lorenzo Martinez[61], M. Losada[163], P. Loscutoff[15], X. Lou[33a], A. Lounis[117], J. Love[6], P.A. Love[72], A.J. Lowe[144,e], F. Lu[33a], N. Lu[89], H.J. Lubatti[139], C. Luci[133a,133b], A. Lucotte[55], F. Luehring[61], W. Lukas[62], L. Luminari[133a], O. Lundberg[147a,147b], B. Lund-Jensen[148], M. Lungwitz[83], D. Lynn[25], R. Lysak[127], E. Lytken[81], H. Ma[25], L.L. Ma[33d], G. Maccarrone[47], A. Macchiolo[101], J. Machado Miguens[126a,126b], D. Macina[30], D. Madaffari[85], R. Madar[48], H.J. Maddocks[72], W.F. Mader[44], A. Madsen[167], M. Maeno[8], T. Maeno[25], A. Maevskiy[99], E. Magradze[54], K. Mahboubi[48], J. Mahlstedt[107], S. Mahmoud[74], C. Maiani[137], C. Maidantchik[24a], A.A. Maier[101], A. Maio[126a,126b,126d], S. Majewski[116], Y. Makida[66], N. Makovec[117], P. Mal[137,y], B. Malaescu[80], Pa. Malecki[39], V.P. Maleev[123], F. Malek[55], U. Mallik[63],

D. Malon[6], C. Malone[144], S. Maltezos[10], V.M. Malyshev[109], S. Malyukov[30], J. Mamuzic[13b], B. Mandelli[30], L. Mandelli[91a], I. Mandić[75], R. Mandrysch[63], J. Maneira[126a,126b], A. Manfredini[101], L. Manhaes de Andrade Filho[24b], J. Manjarres Ramos[160b], A. Mann[100], P.M. Manning[138], A. Manousakis-Katsikakis[9], B. Mansoulie[137], R. Mantifel[87], M. Mantoani[54], L. Mapelli[30], L. March[146c], J.F. Marchand[29], G. Marchiori[80], M. Marcisovsky[127], C.P. Marino[170], M. Marjanovic[13a], F. Marroquim[24a], S.P. Marsden[84], Z. Marshall[15], L.F. Marti[17], S. Marti-Garcia[168], B. Martin[30], B. Martin[90], T.A. Martin[171], V.J. Martin[46], B. Martin dit Latour[14], H. Martinez[137], M. Martinez[12,n], S. Martin-Haugh[131], A.C. Martyniuk[78], M. Marx[139], F. Marzano[133a], A. Marzin[30], L. Masetti[83], T. Mashimo[156], R. Mashinistov[96], J. Masik[84], A.L. Maslennikov[109,c], I. Massa[20a,20b], L. Massa[20a,20b], N. Massol[5], P. Mastrandrea[149], A. Mastroberardino[37a,37b], T. Masubuchi[156], P. Mättig[176], J. Mattmann[83], J. Maurer[26a], S.J. Maxfield[74], D.A. Maximov[109,c], R. Mazini[152], S.M. Mazza[91a,91b], L. Mazzaferro[134a,134b], G. Mc Goldrick[159], S.P. Mc Kee[89], A. McCarn[89], R.L. McCarthy[149], T.G. McCarthy[29], N.A. McCubbin[131], K.W. McFarlane[56,*], J.A. Mcfayden[78], G. Mchedlidze[54], S.J. McMahon[131], R.A. McPherson[170,j], J. Mechnich[107], M. Medinnis[42], S. Meehan[31], S. Mehlhase[100], A. Mehta[74], K. Meier[58a], C. Meineck[100], B. Meirose[41], C. Melachrinos[31], B.R. Mellado Garcia[146c], F. Meloni[17], A. Mengarelli[20a,20b], S. Menke[101], E. Meoni[162], K.M. Mercurio[57], S. Mergelmeyer[21], N. Meric[137], P. Mermod[49], L. Merola[104a,104b], C. Meroni[91a], F.S. Merritt[31], H. Merritt[111], A. Messina[30,z], J. Metcalfe[25], A.S. Mete[164], C. Meyer[83], C. Meyer[122], J-P. Meyer[137], J. Meyer[30], R.P. Middleton[131], S. Migas[74], S. Miglioranzi[165a,165c], L. Mijović[21], G. Mikenberg[173], M. Mikestikova[127], M. Mikuž[75], A. Milic[30], D.W. Miller[31], C. Mills[46], A. Milov[173], D.A. Milstead[147a,147b], A.A. Minaenko[130], Y. Minami[156], I.A. Minashvili[65], A.I. Mincer[110], B. Mindur[38a], M. Mineev[65], Y. Ming[174], L.M. Mir[12], G. Mirabelli[133a], T. Mitani[172], J. Mitrevski[100], V.A. Mitsou[168], A. Miucci[49], P.S. Miyagawa[140], J.U. Mjörnmark[81], T. Moa[147a,147b], K. Mochizuki[85], S. Mohapatra[35], W. Mohr[48], S. Molander[147a,147b], R. Moles-Valls[168], K. Mönig[42], C. Monini[55], J. Monk[36], E. Monnier[85], J. Montejo Berlingen[12], F. Monticelli[71], S. Monzani[133a,133b], R.W. Moore[3], N. Morange[63], D. Moreno[163], M. Moreno Llácer[54], P. Morettini[50a], M. Morgenstern[44], M. Morii[57], V. Morisbak[119], S. Moritz[83], A.K. Morley[148], G. Mornacchi[30], J.D. Morris[76], A. Morton[42], L. Morvaj[103], H.G. Moser[101], M. Mosidze[51b], J. Moss[111], K. Motohashi[158], R. Mount[144], E. Mountricha[25], S.V. Mouraviev[96,*], E.J.W. Moyse[86], S. Muanza[85], R.D. Mudd[18], F. Mueller[58a], J. Mueller[125], K. Mueller[21], T. Mueller[28], D. Muenstermann[49], P. Mullen[53], Y. Munwes[154], J.A. Murillo Quijada[18], W.J. Murray[171,131], H. Musheghyan[54], E. Musto[153], A.G. Myagkov[130,aa], M. Myska[128], O. Nackenhorst[54], J. Nadal[54], K. Nagai[120], R. Nagai[158], Y. Nagai[85], K. Nagano[66], A. Nagarkar[111], Y. Nagasaka[59], K. Nagata[161], M. Nagel[101], A.M. Nairz[30], Y. Nakahama[30], K. Nakamura[66], T. Nakamura[156], I. Nakano[112], H. Namasivayam[41], G. Nanava[21], R.F. Naranjo Garcia[42], R. Narayan[58b], T. Nattermann[21], T. Naumann[42], G. Navarro[163], R. Nayyar[7], H.A. Neal[89], P.Yu. Nechaeva[96], T.J. Neep[84], P.D. Nef[144], A. Negri[121a,121b], G. Negri[30], M. Negrini[20a], S. Nektarijevic[49], C. Nellist[117], A. Nelson[164], T.K. Nelson[144], S. Nemecek[127], P. Nemethy[110], A.A. Nepomuceno[24a], M. Nessi[30,ab],

M.S. Neubauer[166], M. Neumann[176], R.M. Neves[110], P. Nevski[25], P.R. Newman[18], D.H. Nguyen[6], R.B. Nickerson[120], R. Nicolaidou[137], B. Nicquevert[30], J. Nielsen[138], N. Nikiforou[35], A. Nikiforov[16], V. Nikolaenko[130,aa], I. Nikolic-Audit[80], K. Nikolics[49], K. Nikolopoulos[18], P. Nilsson[25], Y. Ninomiya[156], A. Nisati[133a], R. Nisius[101], T. Nobe[158], M. Nomachi[118], I. Nomidis[29], S. Norberg[113], M. Nordberg[30], O. Novgorodova[44], S. Nowak[101], M. Nozaki[66], L. Nozka[115], K. Ntekas[10], G. Nunes Hanninger[88], T. Nunnemann[100], E. Nurse[78], F. Nuti[88], B.J. O'Brien[46], F. O'grady[7], D.C. O'Neil[143], V. O'Shea[53], F.G. Oakham[29,d], H. Oberlack[101], T. Obermann[21], J. Ocariz[80], A. Ochi[67], I. Ochoa[78], S. Oda[70], S. Odaka[66], H. Ogren[61], A. Oh[84], S.H. Oh[45], C.C. Ohm[15], H. Ohman[167], H. Oide[30], W. Okamura[118], H. Okawa[161], Y. Okumura[31], T. Okuyama[156], A. Olariu[26a], A.G. Olchevski[65], S.A. Olivares Pino[46], D. Oliveira Damazio[25], E. Oliver Garcia[168], A. Olszewski[39], J. Olszowska[39], A. Onofre[126a,126e], P.U.E. Onyisi[31,p], C.J. Oram[160a], M.J. Oreglia[31], Y. Oren[154], D. Orestano[135a,135b], N. Orlando[73a,73b], C. Oropeza Barrera[53], R.S. Orr[159], B. Osculati[50a,50b], R. Ospanov[122], G. Otero y Garzon[27], H. Otono[70], M. Ouchrif[136d], E.A. Ouellette[170], F. Ould-Saada[119], A. Ouraou[137], K.P. Oussoren[107], Q. Ouyang[33a], A. Ovcharova[15], M. Owen[84], V.E. Ozcan[19a], N. Ozturk[8], K. Pachal[120], A. Pacheco Pages[12], C. Padilla Aranda[12], M. Pagáčová[48], S. Pagan Griso[15], E. Paganis[140], C. Pahl[101], F. Paige[25], P. Pais[86], K. Pajchel[119], G. Palacino[160b], S. Palestini[30], M. Palka[38b], D. Pallin[34], A. Palma[126a,126b], J.D. Palmer[18], Y.B. Pan[174], E. Panagiotopoulou[10], J.G. Panduro Vazquez[77], P. Pani[107], N. Panikashvili[89], S. Panitkin[25], D. Pantea[26a], L. Paolozzi[134a,134b], Th.D. Papadopoulou[10], K. Papageorgiou[155], A. Paramonov[6], D. Paredes Hernandez[155], M.A. Parker[28], F. Parodi[50a,50b], J.A. Parsons[35], U. Parzefall[48], E. Pasqualucci[133a], S. Passaggio[50a], A. Passeri[135a], F. Pastore[135a,135b,*], Fr. Pastore[77], G. Pásztor[29], S. Pataraia[176], N.D. Patel[151], J.R. Pater[84], S. Patricelli[104a,104b], T. Pauly[30], J. Pearce[170], L.E. Pedersen[36], M. Pedersen[119], S. Pedraza Lopez[168], R. Pedro[126a,126b], S.V. Peleganchuk[109], D. Pelikan[167], H. Peng[33b], B. Penning[31], J. Penwell[61], D.V. Perepelitsa[25], E. Perez Codina[160a], M.T. Pérez García-Estañ[168], L. Perini[91a,91b], H. Pernegger[30], S. Perrella[104a,104b], R. Peschke[42], V.D. Peshekhonov[65], K. Peters[30], R.F.Y. Peters[84], B.A. Petersen[30], T.C. Petersen[36], E. Petit[42], A. Petridis[147a,147b], C. Petridou[155], E. Petrolo[133a], F. Petrucci[135a,135b], N.E. Pettersson[158], R. Pezoa[32b], P.W. Phillips[131], G. Piacquadio[144], E. Pianori[171], A. Picazio[49], E. Piccaro[76], M. Piccinini[20a,20b], M.A. Pickering[120], R. Piegaia[27], D.T. Pignotti[111], J.E. Pilcher[31], A.D. Pilkington[78], J. Pina[126a,126b,126d], M. Pinamonti[165a,165c,ac], A. Pinder[120], J.L. Pinfold[3], A. Pingel[36], B. Pinto[126a], S. Pires[80], M. Pitt[173], C. Pizio[91a,91b], L. Plazak[145a], M.-A. Pleier[25], V. Pleskot[129], E. Plotnikova[65], P. Plucinski[147a,147b], D. Pluth[64], S. Poddar[58a], F. Podlyski[34], R. Poettgen[83], L. Poggioli[117], D. Pohl[21], M. Pohl[49], G. Polesello[121a], A. Policicchio[37a,37b], R. Polifka[159], A. Polini[20a], C.S. Pollard[53], V. Polychronakos[25], K. Pommès[30], L. Pontecorvo[133a], B.G. Pope[90], G.A. Popeneciu[26b], D.S. Popovic[13a], A. Poppleton[30], S. Pospisil[128], K. Potamianos[15], I.N. Potrap[65], C.J. Potter[150], C.T. Potter[116], G. Poulard[30], J. Poveda[30], V. Pozdnyakov[65], P. Pralavorio[85], A. Pranko[15], S. Prasad[30], S. Prell[64], D. Price[84], J. Price[74], L.E. Price[6], D. Prieur[125], M. Primavera[73a], S. Prince[87], M. Proissl[46],

K. Prokofiev[60c], F. Prokoshin[32b], E. Protopapadaki[137], S. Protopopescu[25], J. Proudfoot[6], M. Przybycien[38a], H. Przysiezniak[5], E. Ptacek[116], D. Puddu[135a,135b], E. Pueschel[86], D. Puldon[149], M. Purohit[25,ad], P. Puzo[117], J. Qian[89], G. Qin[53], Y. Qin[84], A. Quadt[54], D.R. Quarrie[15], W.B. Quayle[165a,165b], M. Queitsch-Maitland[84], D. Quilty[53], A. Qureshi[160b], V. Radeka[25], V. Radescu[42], S.K. Radhakrishnan[149], P. Radloff[116], P. Rados[88], F. Ragusa[91a,91b], G. Rahal[179], S. Rajagopalan[25], M. Rammensee[30], C. Rangel-Smith[167], K. Rao[164], F. Rauscher[100], S. Rave[83], T.C. Rave[48], T. Ravenscroft[53], M. Raymond[30], A.L. Read[119], N.P. Readioff[74], D.M. Rebuzzi[121a,121b], A. Redelbach[175], G. Redlinger[25], R. Reece[138], K. Reeves[41], L. Rehnisch[16], H. Reisin[27], M. Relich[164], C. Rembser[30], H. Ren[33a], Z.L. Ren[152], A. Renaud[117], M. Rescigno[133a], S. Resconi[91a], O.L. Rezanova[109,c], P. Reznicek[129], R. Rezvani[95], R. Richter[101], M. Ridel[80], P. Rieck[16], J. Rieger[54], M. Rijssenbeek[149], A. Rimoldi[121a,121b], L. Rinaldi[20a], E. Ritsch[62], I. Riu[12], F. Rizatdinova[114], E. Rizvi[76], S.H. Robertson[87,j], A. Robichaud-Veronneau[87], D. Robinson[28], J.E.M. Robinson[84], A. Robson[53], C. Roda[124a,124b], L. Rodrigues[30], S. Roe[30], O. Røhne[119], S. Rolli[162], A. Romaniouk[98], M. Romano[20a,20b], E. Romero Adam[168], N. Rompotis[139], M. Ronzani[48], L. Roos[80], E. Ros[168], S. Rosati[133a], K. Rosbach[49], M. Rose[77], P. Rose[138], P.L. Rosendahl[14], O. Rosenthal[142], V. Rossetti[147a,147b], E. Rossi[104a,104b], L.P. Rossi[50a], R. Rosten[139], M. Rotaru[26a], I. Roth[173], J. Rothberg[139], D. Rousseau[117], C.R. Royon[137], A. Rozanov[85], Y. Rozen[153], X. Ruan[146c], F. Rubbo[12], I. Rubinskiy[42], V.I. Rud[99], C. Rudolph[44], M.S. Rudolph[159], F. Rühr[48], A. Ruiz-Martinez[30], Z. Rurikova[48], N.A. Rusakovich[65], A. Ruschke[100], H.L. Russell[139], J.P. Rutherfoord[7], N. Ruthmann[48], Y.F. Ryabov[123], M. Rybar[129], G. Rybkin[117], N.C. Ryder[120], A.F. Saavedra[151], G. Sabato[107], S. Sacerdoti[27], A. Saddique[3], H.F-W. Sadrozinski[138], R. Sadykov[65], F. Safai Tehrani[133a], H. Sakamoto[156], Y. Sakurai[172], G. Salamanna[135a,135b], A. Salamon[134a], M. Saleem[113], D. Salek[107], P.H. Sales De Bruin[139], D. Salihagic[101], A. Salnikov[144], J. Salt[168], D. Salvatore[37a,37b], F. Salvatore[150], A. Salvucci[106], A. Salzburger[30], D. Sampsonidis[155], A. Sanchez[104a,104b], J. Sánchez[168], V. Sanchez Martinez[168], H. Sandaker[14], R.L. Sandbach[76], H.G. Sander[83], M.P. Sanders[100], M. Sandhoff[176], T. Sandoval[28], C. Sandoval[163], R. Sandstroem[101], D.P.C. Sankey[131], A. Sansoni[47], C. Santoni[34], R. Santonico[134a,134b], H. Santos[126a], I. Santoyo Castillo[150], K. Sapp[125], A. Sapronov[65], J.G. Saraiva[126a,126d], B. Sarrazin[21], G. Sartisohn[176], O. Sasaki[66], Y. Sasaki[156], K. Sato[161], G. Sauvage[5,*], E. Sauvan[5], P. Savard[159,d], D.O. Savu[30], C. Sawyer[120], L. Sawyer[79,m], D.H. Saxon[53], J. Saxon[31], C. Sbarra[20a], A. Sbrizzi[20a,20b], T. Scanlon[78], D.A. Scannicchio[164], M. Scarcella[151], V. Scarfone[37a,37b], J. Schaarschmidt[173], P. Schacht[101], D. Schaefer[30], R. Schaefer[42], S. Schaepe[21], S. Schaetzel[58b], U. Schäfer[83], A.C. Schaffer[117], D. Schaile[100], R.D. Schamberger[149], V. Scharf[58a], V.A. Schegelsky[123], D. Scheirich[129], M. Schernau[164], C. Schiavi[50a,50b], J. Schieck[100], C. Schillo[48], M. Schioppa[37a,37b], S. Schlenker[30], E. Schmidt[48], K. Schmieden[30], C. Schmitt[83], S. Schmitt[58b], B. Schneider[17], Y.J. Schnellbach[74], U. Schnoor[44], L. Schoeffel[137], A. Schoening[58b], B.D. Schoenrock[90], A.L.S. Schorlemmer[54], M. Schott[83], D. Schouten[160a], J. Schovancova[25], S. Schramm[159], M. Schreyer[175], C. Schroeder[83], N. Schuh[83], M.J. Schultens[21], H.-C. Schultz-Coulon[58a], H. Schulz[16], M. Schumacher[48],

B.A. Schumm[138], Ph. Schune[137], C. Schwanenberger[84], A. Schwartzman[144], T.A. Schwarz[89], Ph. Schwegler[101], Ph. Schwemling[137], R. Schwienhorst[90], J. Schwindling[137], T. Schwindt[21], M. Schwoerer[5], F.G. Sciacca[17], E. Scifo[117], G. Sciolla[23], F. Scuri[124a,124b], F. Scutti[21], J. Searcy[89], G. Sedov[42], E. Sedykh[123], P. Seema[21], S.C. Seidel[105], A. Seiden[138], F. Seifert[128], J.M. Seixas[24a], G. Sekhniaidze[104a], S.J. Sekula[40], K.E. Selbach[46], D.M. Seliverstov[123,*], G. Sellers[74], N. Semprini-Cesari[20a,20b], C. Serfon[30], L. Serin[117], L. Serkin[54], T. Serre[85], R. Seuster[160a], H. Severini[113], T. Sfiligoj[75], F. Sforza[101], A. Sfyrla[30], E. Shabalina[54], M. Shamim[116], L.Y. Shan[33a], R. Shang[166], J.T. Shank[22], M. Shapiro[15], P.B. Shatalov[97], K. Shaw[165a,165b], A. Shcherbakova[147a,147b], C.Y. Shehu[150], P. Sherwood[78], L. Shi[152,ae], S. Shimizu[67], C.O. Shimmin[164], M. Shimojima[102], M. Shiyakova[65], A. Shmeleva[96], D. Shoaleh Saadi[95], M.J. Shochet[31], S. Shojaii[91a,91b], D. Short[120], S. Shrestha[111], E. Shulga[98], M.A. Shupe[7], S. Shushkevich[42], P. Sicho[127], O. Sidiropoulou[155], D. Sidorov[114], A. Sidoti[133a], F. Siegert[44], Dj. Sijacki[13a], J. Silva[126a,126d], Y. Silver[154], D. Silverstein[144], S.B. Silverstein[147a], V. Simak[128], O. Simard[5], Lj. Simic[13a], S. Simion[117], E. Simioni[83], B. Simmons[78], D. Simon[34], R. Simoniello[91a,91b], P. Sinervo[159], N.B. Sinev[116], G. Siragusa[175], A. Sircar[79], A.N. Sisakyan[65,*], S.Yu. Sivoklokov[99], J. Sjölin[147a,147b], T.B. Sjursen[14], H.P. Skottowe[57], P. Skubic[113], M. Slater[18], T. Slavicek[128], M. Slawinska[107], K. Sliwa[162], V. Smakhtin[173], B.H. Smart[46], L. Smestad[14], S.Yu. Smirnov[98], Y. Smirnov[98], L.N. Smirnova[99,af], O. Smirnova[81], K.M. Smith[53], M. Smizanska[72], K. Smolek[128], A.A. Snesarev[96], G. Snidero[76], S. Snyder[25], R. Sobie[170,j], F. Socher[44], A. Soffer[154], D.A. Soh[152,ae], C.A. Solans[30], M. Solar[128], J. Solc[128], E.Yu. Soldatov[98], U. Soldevila[168], A.A. Solodkov[130], A. Soloshenko[65], O.V. Solovyanov[130], V. Solovyev[123], P. Sommer[48], H.Y. Song[33b], N. Soni[1], A. Sood[15], A. Sopczak[128], B. Sopko[128], V. Sopko[128], V. Sorin[12], M. Sosebee[8], R. Soualah[165a,165c], P. Soueid[95], A.M. Soukharev[109,c], D. South[42], S. Spagnolo[73a,73b], F. Spanò[77], W.R. Spearman[57], F. Spettel[101], R. Spighi[20a], G. Spigo[30], L.A. Spiller[88], M. Spousta[129], T. Spreitzer[159], R.D. St. Denis[53,*], S. Staerz[44], J. Stahlman[122], R. Stamen[58a], S. Stamm[16], E. Stanecka[39], C. Stanescu[135a], M. Stanescu-Bellu[42], M.M. Stanitzki[42], S. Stapnes[119], E.A. Starchenko[130], J. Stark[55], P. Staroba[127], P. Starovoitov[42], R. Staszewski[39], P. Stavina[145a,*], P. Steinberg[25], B. Stelzer[143], H.J. Stelzer[30], O. Stelzer-Chilton[160a], H. Stenzel[52], S. Stern[101], G.A. Stewart[53], J.A. Stillings[21], M.C. Stockton[87], M. Stoebe[87], G. Stoicea[26a], P. Stolte[54], S. Stonjek[101], A.R. Stradling[8], A. Straessner[44], M.E. Stramaglia[17], J. Strandberg[148], S. Strandberg[147a,147b], A. Strandlie[119], E. Strauss[144], M. Strauss[113], P. Strizenec[145b], R. Ströhmer[175], D.M. Strom[116], R. Stroynowski[40], A. Strubig[106], S.A. Stucci[17], B. Stugu[14], N.A. Styles[42], D. Su[144], J. Su[125], R. Subramaniam[79], A. Succurro[12], Y. Sugaya[118], C. Suhr[108], M. Suk[128], V.V. Sulin[96], S. Sultansoy[4d], T. Sumida[68], S. Sun[57], X. Sun[33a], J.E. Sundermann[48], K. Suruliz[150], G. Susinno[37a,37b], M.R. Sutton[150], Y. Suzuki[66], M. Svatos[127], S. Swedish[169], M. Swiatlowski[144], I. Sykora[145a], T. Sykora[129], D. Ta[90], C. Taccini[135a,135b], K. Tackmann[42], J. Taenzer[159], A. Taffard[164], R. Tafirout[160a], N. Taiblum[154], H. Takai[25], R. Takashima[69], H. Takeda[67], T. Takeshita[141], Y. Takubo[66], M. Talby[85], A.A. Talyshev[109,c], J.Y.C. Tam[175], K.G. Tan[88], J. Tanaka[156], R. Tanaka[117],

S. Tanaka[132], S. Tanaka[66], A.J. Tanasijczuk[143], B.B. Tannenwald[111], N. Tannoury[21], S. Tapprogge[83], S. Tarem[153], F. Tarrade[29], G.F. Tartarelli[91a], P. Tas[129], M. Tasevsky[127], T. Tashiro[68], E. Tassi[37a,37b], A. Tavares Delgado[126a,126b], Y. Tayalati[136d], F.E. Taylor[94], G.N. Taylor[88], W. Taylor[160b], F.A. Teischinger[30], M. Teixeira Dias Castanheira[76], P. Teixeira-Dias[77], K.K. Temming[48], H. Ten Kate[30], P.K. Teng[152], J.J. Teoh[118], F. Tepel[176], S. Terada[66], K. Terashi[156], J. Terron[82], S. Terzo[101], M. Testa[47], R.J. Teuscher[159,j], J. Therhaag[21], T. Theveneaux-Pelzer[34], J.P. Thomas[18], J. Thomas-Wilsker[77], E.N. Thompson[35], P.D. Thompson[18], R.J. Thompson[84], A.S. Thompson[53], L.A. Thomsen[36], E. Thomson[122], M. Thomson[28], W.M. Thong[88], R.P. Thun[89,*], F. Tian[35], M.J. Tibbetts[15], V.O. Tikhomirov[96,ag], Yu.A. Tikhonov[109,c], S. Timoshenko[98], E. Tiouchichine[85], P. Tipton[177], S. Tisserant[85], T. Todorov[5,*], S. Todorova-Nova[129], J. Tojo[70], S. Tokár[145a], K. Tokushuku[66], K. Tollefson[90], E. Tolley[57], L. Tomlinson[84], M. Tomoto[103], L. Tompkins[31], K. Toms[105], N.D. Topilin[65], E. Torrence[116], H. Torres[143], E. Torró Pastor[168], J. Toth[85,ah], F. Touchard[85], D.R. Tovey[140], H.L. Tran[117], T. Trefzger[175], L. Tremblet[30], A. Tricoli[30], I.M. Trigger[160a], S. Trincaz-Duvoid[80], M.F. Tripiana[12], W. Trischuk[159], B. Trocmé[55], C. Troncon[91a], M. Trottier-McDonald[15], M. Trovatelli[135a,135b], P. True[90], M. Trzebinski[39], A. Trzupek[39], C. Tsarouchas[30], J.C-L. Tseng[120], P.V. Tsiareshka[92], D. Tsionou[137], G. Tsipolitis[10], N. Tsirintanis[9], S. Tsiskaridze[12], V. Tsiskaridze[48], E.G. Tskhadadze[51a], I.I. Tsukerman[97], V. Tsulaia[15], S. Tsuno[66], D. Tsybychev[149], A. Tudorache[26a], V. Tudorache[26a], A.N. Tuna[122], S.A. Tupputi[20a,20b], S. Turchikhin[99,af], D. Turecek[128], I. Turk Cakir[4c], R. Turra[91a,91b], A.J. Turvey[40], P.M. Tuts[35], A. Tykhonov[49], M. Tylmad[147a,147b], M. Tyndel[131], I. Ueda[156], R. Ueno[29], M. Ughetto[85], M. Ugland[14], M. Uhlenbrock[21], F. Ukegawa[161], G. Unal[30], A. Undrus[25], G. Unel[164], F.C. Ungaro[48], Y. Unno[66], C. Unverdorben[100], J. Urban[145b], D. Urbaniec[35], P. Urquijo[88], G. Usai[8], A. Usanova[62], L. Vacavant[85], V. Vacek[128], B. Vachon[87], N. Valencic[107], S. Valentinetti[20a,20b], A. Valero[168], L. Valery[34], S. Valkar[129], E. Valladolid Gallego[168], S. Vallecorsa[49], J.A. Valls Ferrer[168], W. Van Den Wollenberg[107], P.C. Van Der Deijl[107], R. van der Geer[107], H. van der Graaf[107], R. Van Der Leeuw[107], D. van der Ster[30], N. van Eldik[30], P. van Gemmeren[6], J. Van Nieuwkoop[143], I. van Vulpen[107], M.C. van Woerden[30], M. Vanadia[133a,133b], W. Vandelli[30], R. Vanguri[122], A. Vaniachine[6], P. Vankov[42], F. Vannucci[80], G. Vardanyan[178], R. Vari[133a], E.W. Varnes[7], T. Varol[86], D. Varouchas[80], A. Vartapetian[8], K.E. Varvell[151], F. Vazeille[34], T. Vazquez Schroeder[54], J. Veatch[7], F. Veloso[126a,126c], T. Velz[21], S. Veneziano[133a], A. Ventura[73a,73b], D. Ventura[86], M. Venturi[170], N. Venturi[159], A. Venturini[23], V. Vercesi[121a], M. Verducci[133a,133b], W. Verkerke[107], J.C. Vermeulen[107], A. Vest[44], M.C. Vetterli[143,d], O. Viazlo[81], I. Vichou[166], T. Vickey[146c,ai], O.E. Vickey Boeriu[146c], G.H.A. Viehhauser[120], S. Viel[169], R. Vigne[30], M. Villa[20a,20b], M. Villaplana Perez[91a,91b], E. Vilucchi[47], M.G. Vincter[29], V.B. Vinogradov[65], J. Virzi[15], I. Vivarelli[150], F. Vives Vaque[3], S. Vlachos[10], D. Vladoiu[100], M. Vlasak[128], A. Vogel[21], M. Vogel[32a], P. Vokac[128], G. Volpi[124a,124b], M. Volpi[88], H. von der Schmitt[101], H. von Radziewski[48], E. von Toerne[21], V. Vorobel[129], K. Vorobev[98], M. Vos[168], R. Voss[30], J.H. Vossebeld[74], N. Vranjes[137], M. Vranjes Milosavljevic[13a], V. Vrba[127], M. Vreeswijk[107], T. Vu Anh[48],

R. Vuillermet[30], I. Vukotic[31], Z. Vykydal[128], P. Wagner[21], W. Wagner[176], H. Wahlberg[71], S. Wahrmund[44], J. Wakabayashi[103], J. Walder[72], R. Walker[100], W. Walkowiak[142], R. Wall[177], P. Waller[74], B. Walsh[177], C. Wang[33c], C. Wang[45], F. Wang[174], H. Wang[15], H. Wang[40], J. Wang[42], J. Wang[33a], K. Wang[87], R. Wang[105], S.M. Wang[152], T. Wang[21], X. Wang[177], C. Wanotayaroj[116], A. Warburton[87], C.P. Ward[28], D.R. Wardrope[78], M. Warsinsky[48], A. Washbrook[46], C. Wasicki[42], P.M. Watkins[18], A.T. Watson[18], I.J. Watson[151], M.F. Watson[18], G. Watts[139], S. Watts[84], B.M. Waugh[78], S. Webb[84], M.S. Weber[17], S.W. Weber[175], J.S. Webster[31], A.R. Weidberg[120], B. Weinert[61], J. Weingarten[54], C. Weiser[48], H. Weits[107], P.S. Wells[30], T. Wenaus[25], D. Wendland[16], Z. Weng[152,ae], T. Wengler[30], S. Wenig[30], N. Wermes[21], M. Werner[48], P. Werner[30], M. Wessels[58a], J. Wetter[162], K. Whalen[29], A. White[8], M.J. White[1], R. White[32b], S. White[124a,124b], D. Whiteson[164], D. Wicke[176], F.J. Wickens[131], W. Wiedenmann[174], M. Wielers[131], P. Wienemann[21], C. Wiglesworth[36], L.A.M. Wiik-Fuchs[21], P.A. Wijeratne[78], A. Wildauer[101], M.A. Wildt[42,aj], H.G. Wilkens[30], H.H. Williams[122], S. Williams[28], C. Willis[90], S. Willocq[86], A. Wilson[89], J.A. Wilson[18], I. Wingerter-Seez[5], F. Winklmeier[116], B.T. Winter[21], M. Wittgen[144], J. Wittkowski[100], S.J. Wollstadt[83], M.W. Wolter[39], H. Wolters[126a,126c], B.K. Wosiek[39], J. Wotschack[30], M.J. Woudstra[84], K.W. Wozniak[39], M. Wright[53], M. Wu[55], S.L. Wu[174], X. Wu[49], Y. Wu[89], T.R. Wyatt[84], B.M. Wynne[46], S. Xella[36], M. Xiao[137], D. Xu[33a], L. Xu[33b,ak], B. Yabsley[151], S. Yacoob[146b,al], R. Yakabe[67], M. Yamada[66], H. Yamaguchi[156], Y. Yamaguchi[118], A. Yamamoto[66], S. Yamamoto[156], T. Yamamura[156], T. Yamanaka[156], K. Yamauchi[103], Y. Yamazaki[67], Z. Yan[22], H. Yang[33e], H. Yang[174], Y. Yang[111], S. Yanush[93], L. Yao[33a], W-M. Yao[15], Y. Yasu[66], E. Yatsenko[42], K.H. Yau Wong[21], J. Ye[40], S. Ye[25], I. Yeletskikh[65], A.L. Yen[57], E. Yildirim[42], M. Yilmaz[4b], R. Yoosoofmiya[125], K. Yorita[172], R. Yoshida[6], K. Yoshihara[156], C. Young[144], C.J.S. Young[30], S. Youssef[22], D.R. Yu[15], J. Yu[8], J.M. Yu[89], J. Yu[114], L. Yuan[67], A. Yurkewicz[108], I. Yusuff[28,am], B. Zabinski[39], R. Zaidan[63], A.M. Zaitsev[130,aa], A. Zaman[149], S. Zambito[23], L. Zanello[133a,133b], D. Zanzi[88], C. Zeitnitz[176], M. Zeman[128], A. Zemla[38a], K. Zengel[23], O. Zenin[130], T. Ženiš[145a], D. Zerwas[117], G. Zevi della Porta[57], D. Zhang[89], F. Zhang[174], H. Zhang[90], J. Zhang[6], L. Zhang[152], R. Zhang[33b], X. Zhang[33d], Z. Zhang[117], X. Zhao[40], Y. Zhao[33d], Z. Zhao[33b], A. Zhemchugov[65], J. Zhong[120], B. Zhou[89], L. Zhou[35], L. Zhou[40], N. Zhou[164], C.G. Zhu[33d], H. Zhu[33a], J. Zhu[89], Y. Zhu[33b], X. Zhuang[33a], K. Zhukov[96], A. Zibell[175], D. Zieminska[61], N.I. Zimine[65], C. Zimmermann[83], R. Zimmermann[21], S. Zimmermann[21], S. Zimmermann[48], Z. Zinonos[54], M. Ziolkowski[142], G. Zobernig[174], A. Zoccoli[20a,20b], M. zur Nedden[16], G. Zurzolo[104a,104b], L. Zwalinski[30].

[1] Department of Physics, University of Adelaide, Adelaide, Australia
[2] Physics Department, SUNY Albany, Albany NY, United States of America
[3] Department of Physics, University of Alberta, Edmonton AB, Canada
[4] (a) Department of Physics, Ankara University, Ankara; (b) Department of Physics, Gazi University, Ankara; (c) Istanbul Aydin University, Istanbul; (d) Division of Physics, TOBB University of Economics and Technology, Ankara, Turkey
[5] LAPP, CNRS/IN2P3 and Université de Savoie, Annecy-le-Vieux, France

[6] High Energy Physics Division, Argonne National Laboratory, Argonne IL, United States of America
[7] Department of Physics, University of Arizona, Tucson AZ, United States of America
[8] Department of Physics, The University of Texas at Arlington, Arlington TX, United States of America
[9] Physics Department, University of Athens, Athens, Greece
[10] Physics Department, National Technical University of Athens, Zografou, Greece
[11] Institute of Physics, Azerbaijan Academy of Sciences, Baku, Azerbaijan
[12] Institut de Física d'Altes Energies and Departament de Física de la Universitat Autònoma de Barcelona, Barcelona, Spain
[13] [(a)] Institute of Physics, University of Belgrade, Belgrade; [(b)] Vinca Institute of Nuclear Sciences, University of Belgrade, Belgrade, Serbia
[14] Department for Physics and Technology, University of Bergen, Bergen, Norway
[15] Physics Division, Lawrence Berkeley National Laboratory and University of California, Berkeley CA, United States of America
[16] Department of Physics, Humboldt University, Berlin, Germany
[17] Albert Einstein Center for Fundamental Physics and Laboratory for High Energy Physics, University of Bern, Bern, Switzerland
[18] School of Physics and Astronomy, University of Birmingham, Birmingham, United Kingdom
[19] [(a)] Department of Physics, Bogazici University, Istanbul; [(b)] Department of Physics, Dogus University, Istanbul; [(c)] Department of Physics Engineering, Gaziantep University, Gaziantep, Turkey
[20] [(a)] INFN Sezione di Bologna; [(b)] Dipartimento di Fisica e Astronomia, Università di Bologna, Bologna, Italy
[21] Physikalisches Institut, University of Bonn, Bonn, Germany
[22] Department of Physics, Boston University, Boston MA, United States of America
[23] Department of Physics, Brandeis University, Waltham MA, United States of America
[24] [(a)] Universidade Federal do Rio De Janeiro COPPE/EE/IF, Rio de Janeiro; [(b)] Electrical Circuits Department, Federal University of Juiz de Fora (UFJF), Juiz de Fora; [(c)] Federal University of Sao Joao del Rei (UFSJ), Sao Joao del Rei; [(d)] Instituto de Fisica, Universidade de Sao Paulo, Sao Paulo, Brazil
[25] Physics Department, Brookhaven National Laboratory, Upton NY, United States of America
[26] [(a)] National Institute of Physics and Nuclear Engineering, Bucharest; [(b)] National Institute for Research and Development of Isotopic and Molecular Technologies, Physics Department, Cluj Napoca; [(c)] University Politehnica Bucharest, Bucharest; [(d)] West University in Timisoara, Timisoara, Romania
[27] Departamento de Física, Universidad de Buenos Aires, Buenos Aires, Argentina
[28] Cavendish Laboratory, University of Cambridge, Cambridge, United Kingdom
[29] Department of Physics, Carleton University, Ottawa ON, Canada
[30] CERN, Geneva, Switzerland
[31] Enrico Fermi Institute, University of Chicago, Chicago IL, United States of America

[32] [(a)] Departamento de Física, Pontificia Universidad Católica de Chile, Santiago; [(b)] Departamento de Física, Universidad Técnica Federico Santa María, Valparaíso, Chile
[33] [(a)] Institute of High Energy Physics, Chinese Academy of Sciences, Beijing; [(b)] Department of Modern Physics, University of Science and Technology of China, Anhui; [(c)] Department of Physics, Nanjing University, Jiangsu; [(d)] School of Physics, Shandong University, Shandong; [(e)] Physics Department, Shanghai Jiao Tong University, Shanghai; [(f)] Physics Department, Tsinghua University, Beijing 100084, China
[34] Laboratoire de Physique Corpusculaire, Clermont Université and Université Blaise Pascal and CNRS/IN2P3, Clermont-Ferrand, France
[35] Nevis Laboratory, Columbia University, Irvington NY, United States of America
[36] Niels Bohr Institute, University of Copenhagen, Kobenhavn, Denmark
[37] [(a)] INFN Gruppo Collegato di Cosenza, Laboratori Nazionali di Frascati; [(b)] Dipartimento di Fisica, Università della Calabria, Rende, Italy
[38] [(a)] AGH University of Science and Technology, Faculty of Physics and Applied Computer Science, Krakow; [(b)] Marian Smoluchowski Institute of Physics, Jagiellonian University, Krakow, Poland
[39] The Henryk Niewodniczanski Institute of Nuclear Physics, Polish Academy of Sciences, Krakow, Poland
[40] Physics Department, Southern Methodist University, Dallas TX, United States of America
[41] Physics Department, University of Texas at Dallas, Richardson TX, United States of America
[42] DESY, Hamburg and Zeuthen, Germany
[43] Institut für Experimentelle Physik IV, Technische Universität Dortmund, Dortmund, Germany
[44] Institut für Kern- und Teilchenphysik, Technische Universität Dresden, Dresden, Germany
[45] Department of Physics, Duke University, Durham NC, United States of America
[46] SUPA - School of Physics and Astronomy, University of Edinburgh, Edinburgh, United Kingdom
[47] INFN Laboratori Nazionali di Frascati, Frascati, Italy
[48] Fakultät für Mathematik und Physik, Albert-Ludwigs-Universität, Freiburg, Germany
[49] Section de Physique, Université de Genève, Geneva, Switzerland
[50] [(a)] INFN Sezione di Genova; [(b)] Dipartimento di Fisica, Università di Genova, Genova, Italy
[51] [(a)] E. Andronikashvili Institute of Physics, Iv. Javakhishvili Tbilisi State University, Tbilisi; [(b)] High Energy Physics Institute, Tbilisi State University, Tbilisi, Georgia
[52] II Physikalisches Institut, Justus-Liebig-Universität Giessen, Giessen, Germany
[53] SUPA - School of Physics and Astronomy, University of Glasgow, Glasgow, United Kingdom
[54] II Physikalisches Institut, Georg-August-Universität, Göttingen, Germany
[55] Laboratoire de Physique Subatomique et de Cosmologie, Université Grenoble-Alpes, CNRS/IN2P3, Grenoble, France

[56] Department of Physics, Hampton University, Hampton VA, United States of America
[57] Laboratory for Particle Physics and Cosmology, Harvard University, Cambridge MA, United States of America
[58] [(a)] Kirchhoff-Institut für Physik, Ruprecht-Karls-Universität Heidelberg, Heidelberg; [(b)] Physikalisches Institut, Ruprecht-Karls-Universität Heidelberg, Heidelberg; [(c)] ZITI Institut für technische Informatik, Ruprecht-Karls-Universität Heidelberg, Mannheim, Germany
[59] Faculty of Applied Information Science, Hiroshima Institute of Technology, Hiroshima, Japan
[60] [(a)] Department of Physics, The Chinese University of Hong Kong, Shatin, N.T., Hong Kong; [(b)] Department of Physics, The University of Hong Kong, Hong Kong; [(c)] Department of Physics, The Hong Kong University of Science and Technology, Clear Water Bay, Kowloon, Hong Kong, China
[61] Department of Physics, Indiana University, Bloomington IN, United States of America
[62] Institut für Astro- und Teilchenphysik, Leopold-Franzens-Universität, Innsbruck, Austria
[63] University of Iowa, Iowa City IA, United States of America
[64] Department of Physics and Astronomy, Iowa State University, Ames IA, United States of America
[65] Joint Institute for Nuclear Research, JINR Dubna, Dubna, Russia
[66] KEK, High Energy Accelerator Research Organization, Tsukuba, Japan
[67] Graduate School of Science, Kobe University, Kobe, Japan
[68] Faculty of Science, Kyoto University, Kyoto, Japan
[69] Kyoto University of Education, Kyoto, Japan
[70] Department of Physics, Kyushu University, Fukuoka, Japan
[71] Instituto de Física La Plata, Universidad Nacional de La Plata and CONICET, La Plata, Argentina
[72] Physics Department, Lancaster University, Lancaster, United Kingdom
[73] [(a)] INFN Sezione di Lecce; [(b)] Dipartimento di Matematica e Fisica, Università del Salento, Lecce, Italy
[74] Oliver Lodge Laboratory, University of Liverpool, Liverpool, United Kingdom
[75] Department of Physics, Jožef Stefan Institute and University of Ljubljana, Ljubljana, Slovenia
[76] School of Physics and Astronomy, Queen Mary University of London, London, United Kingdom
[77] Department of Physics, Royal Holloway University of London, Surrey, United Kingdom
[78] Department of Physics and Astronomy, University College London, London, United Kingdom
[79] Louisiana Tech University, Ruston LA, United States of America
[80] Laboratoire de Physique Nucléaire et de Hautes Energies, UPMC and Université Paris-Diderot and CNRS/IN2P3, Paris, France
[81] Fysiska institutionen, Lunds universitet, Lund, Sweden
[82] Departamento de Fisica Teorica C-15, Universidad Autonoma de Madrid, Madrid,

Spain
[83] Institut für Physik, Universität Mainz, Mainz, Germany
[84] School of Physics and Astronomy, University of Manchester, Manchester, United Kingdom
[85] CPPM, Aix-Marseille Université and CNRS/IN2P3, Marseille, France
[86] Department of Physics, University of Massachusetts, Amherst MA, United States of America
[87] Department of Physics, McGill University, Montreal QC, Canada
[88] School of Physics, University of Melbourne, Victoria, Australia
[89] Department of Physics, The University of Michigan, Ann Arbor MI, United States of America
[90] Department of Physics and Astronomy, Michigan State University, East Lansing MI, United States of America
[91] [(a)] INFN Sezione di Milano; [(b)] Dipartimento di Fisica, Università di Milano, Milano, Italy
[92] B.I. Stepanov Institute of Physics, National Academy of Sciences of Belarus, Minsk, Republic of Belarus
[93] National Scientific and Educational Centre for Particle and High Energy Physics, Minsk, Republic of Belarus
[94] Department of Physics, Massachusetts Institute of Technology, Cambridge MA, United States of America
[95] Group of Particle Physics, University of Montreal, Montreal QC, Canada
[96] P.N. Lebedev Institute of Physics, Academy of Sciences, Moscow, Russia
[97] Institute for Theoretical and Experimental Physics (ITEP), Moscow, Russia
[98] National Research Nuclear University MEPhI, Moscow, Russia
[99] D.V. Skobeltsyn Institute of Nuclear Physics, M.V. Lomonosov Moscow State University, Moscow, Russia
[100] Fakultät für Physik, Ludwig-Maximilians-Universität München, München, Germany
[101] Max-Planck-Institut für Physik (Werner-Heisenberg-Institut), München, Germany
[102] Nagasaki Institute of Applied Science, Nagasaki, Japan
[103] Graduate School of Science and Kobayashi-Maskawa Institute, Nagoya University, Nagoya, Japan
[104] [(a)] INFN Sezione di Napoli; [(b)] Dipartimento di Fisica, Università di Napoli, Napoli, Italy
[105] Department of Physics and Astronomy, University of New Mexico, Albuquerque NM, United States of America
[106] Institute for Mathematics, Astrophysics and Particle Physics, Radboud University Nijmegen/Nikhef, Nijmegen, Netherlands
[107] Nikhef National Institute for Subatomic Physics and University of Amsterdam, Amsterdam, Netherlands
[108] Department of Physics, Northern Illinois University, DeKalb IL, United States of America
[109] Budker Institute of Nuclear Physics, SB RAS, Novosibirsk, Russia

[110] Department of Physics, New York University, New York NY, United States of America
[111] Ohio State University, Columbus OH, United States of America
[112] Faculty of Science, Okayama University, Okayama, Japan
[113] Homer L. Dodge Department of Physics and Astronomy, University of Oklahoma, Norman OK, United States of America
[114] Department of Physics, Oklahoma State University, Stillwater OK, United States of America
[115] Palacký University, RCPTM, Olomouc, Czech Republic
[116] Center for High Energy Physics, University of Oregon, Eugene OR, United States of America
[117] LAL, Université Paris-Sud and CNRS/IN2P3, Orsay, France
[118] Graduate School of Science, Osaka University, Osaka, Japan
[119] Department of Physics, University of Oslo, Oslo, Norway
[120] Department of Physics, Oxford University, Oxford, United Kingdom
[121] [(a)] INFN Sezione di Pavia; [(b)] Dipartimento di Fisica, Università di Pavia, Pavia, Italy
[122] Department of Physics, University of Pennsylvania, Philadelphia PA, United States of America
[123] Petersburg Nuclear Physics Institute, Gatchina, Russia
[124] [(a)] INFN Sezione di Pisa; [(b)] Dipartimento di Fisica E. Fermi, Università di Pisa, Pisa, Italy
[125] Department of Physics and Astronomy, University of Pittsburgh, Pittsburgh PA, United States of America
[126] [(a)] Laboratorio de Instrumentacao e Fisica Experimental de Particulas - LIP, Lisboa; [(b)] Faculdade de Ciências, Universidade de Lisboa, Lisboa; [(c)] Department of Physics, University of Coimbra, Coimbra; [(d)] Centro de Física Nuclear da Universidade de Lisboa, Lisboa; [(e)] Departamento de Fisica, Universidade do Minho, Braga; [(f)] Departamento de Fisica Teorica y del Cosmos and CAFPE, Universidad de Granada, Granada (Spain); [(g)] Dep Fisica and CEFITEC of Faculdade de Ciencias e Tecnologia, Universidade Nova de Lisboa, Caparica, Portugal
[127] Institute of Physics, Academy of Sciences of the Czech Republic, Praha, Czech Republic
[128] Czech Technical University in Prague, Praha, Czech Republic
[129] Faculty of Mathematics and Physics, Charles University in Prague, Praha, Czech Republic
[130] State Research Center Institute for High Energy Physics, Protvino, Russia
[131] Particle Physics Department, Rutherford Appleton Laboratory, Didcot, United Kingdom
[132] Ritsumeikan University, Kusatsu, Shiga, Japan
[133] [(a)] INFN Sezione di Roma; [(b)] Dipartimento di Fisica, Sapienza Università di Roma, Roma, Italy
[134] [(a)] INFN Sezione di Roma Tor Vergata; [(b)] Dipartimento di Fisica, Università di Roma Tor Vergata, Roma, Italy
[135] [(a)] INFN Sezione di Roma Tre; [(b)] Dipartimento di Matematica e Fisica, Università

Roma Tre, Roma, Italy
[136] [(a)] Faculté des Sciences Ain Chock, Réseau Universitaire de Physique des Hautes Energies - Université Hassan II, Casablanca; [(b)] Centre National de l'Energie des Sciences Techniques Nucleaires, Rabat; [(c)] Faculté des Sciences Semlalia, Université Cadi Ayyad, LPHEA-Marrakech; [(d)] Faculté des Sciences, Université Mohamed Premier and LPTPM, Oujda; [(e)] Faculté des sciences, Université Mohammed V-Agdal, Rabat, Morocco
[137] DSM/IRFU (Institut de Recherches sur les Lois Fondamentales de l'Univers), CEA Saclay (Commissariat à l'Energie Atomique et aux Energies Alternatives), Gif-sur-Yvette, France
[138] Santa Cruz Institute for Particle Physics, University of California Santa Cruz, Santa Cruz CA, United States of America
[139] Department of Physics, University of Washington, Seattle WA, United States of America
[140] Department of Physics and Astronomy, University of Sheffield, Sheffield, United Kingdom
[141] Department of Physics, Shinshu University, Nagano, Japan
[142] Fachbereich Physik, Universität Siegen, Siegen, Germany
[143] Department of Physics, Simon Fraser University, Burnaby BC, Canada
[144] SLAC National Accelerator Laboratory, Stanford CA, United States of America
[145] [(a)] Faculty of Mathematics, Physics & Informatics, Comenius University, Bratislava; [(b)] Department of Subnuclear Physics, Institute of Experimental Physics of the Slovak Academy of Sciences, Kosice, Slovak Republic
[146] [(a)] Department of Physics, University of Cape Town, Cape Town; [(b)] Department of Physics, University of Johannesburg, Johannesburg; [(c)] School of Physics, University of the Witwatersrand, Johannesburg, South Africa
[147] [(a)] Department of Physics, Stockholm University; [(b)] The Oskar Klein Centre, Stockholm, Sweden
[148] Physics Department, Royal Institute of Technology, Stockholm, Sweden
[149] Departments of Physics & Astronomy and Chemistry, Stony Brook University, Stony Brook NY, United States of America
[150] Department of Physics and Astronomy, University of Sussex, Brighton, United Kingdom
[151] School of Physics, University of Sydney, Sydney, Australia
[152] Institute of Physics, Academia Sinica, Taipei, Taiwan
[153] Department of Physics, Technion: Israel Institute of Technology, Haifa, Israel
[154] Raymond and Beverly Sackler School of Physics and Astronomy, Tel Aviv University, Tel Aviv, Israel
[155] Department of Physics, Aristotle University of Thessaloniki, Thessaloniki, Greece
[156] International Center for Elementary Particle Physics and Department of Physics, The University of Tokyo, Tokyo, Japan
[157] Graduate School of Science and Technology, Tokyo Metropolitan University, Tokyo, Japan
[158] Department of Physics, Tokyo Institute of Technology, Tokyo, Japan

[159] Department of Physics, University of Toronto, Toronto ON, Canada
[160] [(a)] TRIUMF, Vancouver BC; [(b)] Department of Physics and Astronomy, York University, Toronto ON, Canada
[161] Faculty of Pure and Applied Sciences, University of Tsukuba, Tsukuba, Japan
[162] Department of Physics and Astronomy, Tufts University, Medford MA, United States of America
[163] Centro de Investigaciones, Universidad Antonio Narino, Bogota, Colombia
[164] Department of Physics and Astronomy, University of California Irvine, Irvine CA, United States of America
[165] [(a)] INFN Gruppo Collegato di Udine, Sezione di Trieste, Udine; [(b)] ICTP, Trieste; [(c)] Dipartimento di Chimica, Fisica e Ambiente, Università di Udine, Udine, Italy
[166] Department of Physics, University of Illinois, Urbana IL, United States of America
[167] Department of Physics and Astronomy, University of Uppsala, Uppsala, Sweden
[168] Instituto de Física Corpuscular (IFIC) and Departamento de Física Atómica, Molecular y Nuclear and Departamento de Ingeniería Electrónica and Instituto de Microelectrónica de Barcelona (IMB-CNM), University of Valencia and CSIC, Valencia, Spain
[169] Department of Physics, University of British Columbia, Vancouver BC, Canada
[170] Department of Physics and Astronomy, University of Victoria, Victoria BC, Canada
[171] Department of Physics, University of Warwick, Coventry, United Kingdom
[172] Waseda University, Tokyo, Japan
[173] Department of Particle Physics, The Weizmann Institute of Science, Rehovot, Israel
[174] Department of Physics, University of Wisconsin, Madison WI, United States of America
[175] Fakultät für Physik und Astronomie, Julius-Maximilians-Universität, Würzburg, Germany
[176] Fachbereich C Physik, Bergische Universität Wuppertal, Wuppertal, Germany
[177] Department of Physics, Yale University, New Haven CT, United States of America
[178] Yerevan Physics Institute, Yerevan, Armenia
[179] Centre de Calcul de l'Institut National de Physique Nucléaire et de Physique des Particules (IN2P3), Villeurbanne, France
[a] Also at Department of Physics, King's College London, London, United Kingdom
[b] Also at Institute of Physics, Azerbaijan Academy of Sciences, Baku, Azerbaijan
[c] Also at Novosibirsk State University, Novosibirsk, Russia
[d] Also at TRIUMF, Vancouver BC, Canada
[e] Also at Department of Physics, California State University, Fresno CA, United States of America
[f] Also at Department of Physics, University of Fribourg, Fribourg, Switzerland
[g] Also at Tomsk State University, Tomsk, Russia
[h] Also at CPPM, Aix-Marseille Université and CNRS/IN2P3, Marseille, France
[i] Also at Università di Napoli Parthenope, Napoli, Italy
[j] Also at Institute of Particle Physics (IPP), Canada
[k] Also at Particle Physics Department, Rutherford Appleton Laboratory, Didcot, United

Kingdom
[l] Also at Department of Physics, St. Petersburg State Polytechnical University, St. Petersburg, Russia
[m] Also at Louisiana Tech University, Ruston LA, United States of America
[n] Also at Institucio Catalana de Recerca i Estudis Avancats, ICREA, Barcelona, Spain
[o] Also at Department of Physics, National Tsing Hua University, Taiwan
[p] Also at Department of Physics, The University of Texas at Austin, Austin TX, United States of America
[q] Also at Institute of Theoretical Physics, Ilia State University, Tbilisi, Georgia
[r] Also at CERN, Geneva, Switzerland
[s] Also at Ochadai Academic Production, Ochanomizu University, Tokyo, Japan
[t] Also at Manhattan College, New York NY, United States of America
[u] Also at Institute of Physics, Academia Sinica, Taipei, Taiwan
[v] Also at LAL, Université Paris-Sud and CNRS/IN2P3, Orsay, France
[w] Also at Academia Sinica Grid Computing, Institute of Physics, Academia Sinica, Taipei, Taiwan
[x] Also at Laboratoire de Physique Nucléaire et de Hautes Energies, UPMC and Université Paris-Diderot and CNRS/IN2P3, Paris, France
[y] Also at School of Physical Sciences, National Institute of Science Education and Research, Bhubaneswar, India
[z] Also at Dipartimento di Fisica, Sapienza Università di Roma, Roma, Italy
[aa] Also at Moscow Institute of Physics and Technology State University, Dolgoprudny, Russia
[ab] Also at Section de Physique, Université de Genève, Geneva, Switzerland
[ac] Also at International School for Advanced Studies (SISSA), Trieste, Italy
[ad] Also at Department of Physics and Astronomy, University of South Carolina, Columbia SC, United States of America
[ae] Also at School of Physics and Engineering, Sun Yat-sen University, Guangzhou, China
[af] Also at Faculty of Physics, M.V.Lomonosov Moscow State University, Moscow, Russia
[ag] Also at National Research Nuclear University MEPhI, Moscow, Russia
[ah] Also at Institute for Particle and Nuclear Physics, Wigner Research Centre for Physics, Budapest, Hungary
[ai] Also at Department of Physics, Oxford University, Oxford, United Kingdom
[aj] Also at Institut für Experimentalphysik, Universität Hamburg, Hamburg, Germany
[ak] Also at Department of Physics, The University of Michigan, Ann Arbor MI, United States of America
[al] Also at Discipline of Physics, University of KwaZulu-Natal, Durban, South Africa
[am] Also at University of Malaya, Department of Physics, Kuala Lumpur, Malaysia
* Deceased